





รายงานวิจัยฉบับสมบูรณ์

โครงการการพัฒนาคุณภาพผิวของโลหะผสมโคบอลต์โครเมียม ที่ขึ้นรูปโดยกระบวนการหลอมโดยแสงเลเซอร์ด้วยเทคนิคการ ฉายแสงเลเซอร์ซ้ำ

โดย

อาจารย์ ดร. สุภมาศ สุชาตานนท์ มหาวิทยาลัยธรรมศาสตร์

พฤษภาคม 2561

สัญญาเลขที่ MRG5980217

รายงานวิจัยฉบับสมบูรณ์

โครงการการพัฒนาคุณภาพผิวของโลหะผสม โคบอลต์โครเมียมที่ขึ้นรูปโดยกระบวนการหลอม โดยแสงเลเซอร์ด้วยเทคนิคการฉายแสงเลเซอร์ซ้ำ

> อาจารย์ ดร. สุภมาศ สุชาตานนท์ มหาวิทยาลัยธรรมศาสตร์

สนับสนุนโดยสำนักงานกองทุนสนับสนุนการวิจัย

(ความเห็นในรายงานนี้เป็นของผู้วิจัย สกว. และ สกอ. ไม่จำเป็นต้องเห็นด้วยเสมอไป)

บทคัดย่อ

รหัสโครงการ: MRG5980217

ชื่อโครงการ: การพัฒนาคุณภาพผิวของโลหะผสมโคบอลต์โครเมียมที่ขึ้นรูปโดยกระบวน

การหลอมโดยแสงเลเซอร์ด้วยเทคนิคการฉายแสงเลเซอร์ซ้ำ

ชื่อนักวิจัย: อาจารย์ คร.สุภมาศ สุชาตานนท์

E-mail Address: ssupamar@engr.tu.ac.th

ระยะเวลาโครงการ: 2 พฤษภาคม 2559 ถึง 1 พฤษภาคม 2561

งานวิจัยนี้ ได้มีการนำกระบวนการหลอมซ้ำด้วยเลเซอร์ (Laser re-melting; LRM) มาใช้เพื่อ พัฒนาคุณภาพผิวของ โลหะผสม โคบอลต์ โครเมียมที่ขึ้นรูป โคยกระบวนการหลอม โคยแสงเลเซอร์ (selective laser melting: SLM) โดยมีการปรับปัจจัยของทิศทางการหลอมซ้ำ ปัจจัยของเลเซอร์ และ จำนวนการหลอมซ้ำที่ส่งผลต่อความเรียบผิวของชิ้นงาน SLM ซึ่งจากผลการทคลองในงานวิจัยนี้ได้ พบว่าการหลอมซ้ำนั้นสามารถช่วยให้ลดความหยาบผิวของชิ้นงาน SLM ได้ โดยทิศทางช่วยลด ความหยาบผิว ได้ดีที่สุดนั้นคือทิศทางที่ตั้งฉากกับทิศทางของ SLM และนอกจากนี้ยังพบว่ากำลัง ของเลเซอร์สำหรับการหลอมซ้ำ (Laser re-melting power; P_{LRM}) นั้นควรจะมากกว่าหรือเท่ากับ กำลังที่ใช้ขึ้นรูปชิ้นงาน SLM (P_{SLM}) และความเร็วสำหรับการหลอมซ้ำ (laser re-melting scanning speed; V_{LRM}) ควรเท่ากับความเร็วที่ใช้ขึ้นรูปชิ้นงาน SLM (V_{SLM}) การลดความหยาบผิวให้น้อยลง สามารถทำได้โดยการเพิ่มกำลังของเลเซอร์สำหรับการหลอมซ้ำ ($P_{
m LRM}$) หรือ เพิ่มจำนวนของการ หลอมซ้ำให้มากขึ้น ในการทคลองหลอมซ้ำที่กำลังของเลเซอร์สำหรับการหลอมซ้ำเท่ากับ 150W และความเร็วสำหรับการหลอมซ้ำเท่ากับ 1000 mm/s ได้พบว่าสามารถลดความหยาบผิวของชิ้นงาน SLM ได้จาก 21.99 µm เหลือเพียง 11.98 µm ซึ่งคิดเท่ากับการลดลง 45% ซึ่งถ้าหากทำการหลอมซ้ำ เช่นนี้ซ้ำเป็นจำนวน 3 ครั้งจะทำให้ความหยาบผิวลดลงไปเหลือเพียง 6.49 um ซึ่งเทียบเท่ากับการ ลดลง 70% เมื่อเทียบกับผิวของชิ้นงาน SLM แต่อย่างไรก็ตามกระบวนการหลอมซ้ำด้วยแสงเลเซอร์ ้นั้นจะส่งผลให้ความสูงของชิ้นงานลดลงประมาณ 10 µm แต่อย่างไรก็ตามส่วนต่างนี้สามารถนำไป ้ปรับแต่งในแบบจำนวนก่อนการผลิตชิ้นงานด้วย SLM ภายหลังได้ นอกจากนี้ได้มีการผ่าชิ้นงาน เพื่อศึกษาชั้นผิวของการหลอมซ้ำและได้พบว่าชั้นผิวนี้มีความบางอยู่ที่ต่ำกว่า 200 µm เท่านั้น แต่ อย่างไรก็ตามได้พบว่าค่าความแข็งของชั้นผิวนี้ต่ำกว่าค่าความแข็งของ SLM แต่ยังคงมากกว่าค่า ความแข็งของโลหะผสมโคบอลโครเมียมที่ทำจากการหล่อที่มีขายเชิงพานิชทั่วไป แต่ค่าความแข็ง ของชิ้นงาน LRM ที่แตกต่างไปนั้นอาจส่งผลต่อความสามารถในการต้านทานการสึกหรอได้ ดังนั้น ในงานวิจัยนี้ ใค้มีการศึกษาคณสมบัติการต้านทานการสึกหรอค้วยวิธีบอลออนดิสก์ (ball-on-disk wear test) ของโลหะผสมโคบอลโครเมียมที่ขึ้นรูปโดยการหล่อและวิธี SLM เพื่อเปรียบเทียบกับ ชิ้นงานที่หลอมซ้ำ แต่อย่างไรก็ตามงานวิจัยนี้ไม่สามารถขึ้นรูปชิ้นงานทดสอบการสึกหรอที่ผ่าน การหลอมซ้ำได้ จึงได้ทำการทดสอบเพียงชิ้นงานที่ขึ้นรูปด้วยการหล่อและ SLM ผลการทดลอง พบว่าการต้านทานการสึกหรอของชิ้นงาน SLM นั้นสูงกว่าชิ้นงานที่ทำจากการหล่อ ซึ่งผลนี้ก็ สัมพันธ์กับผลของค่าทดสอบความแข็ง ซึ่งสามารถพยากรณ์ได้ว่าค่าความต้านทานการสึกหรอของ ชิ้นงานที่ผ่านการหลอมซ้ำนั้นอาจมีการต้านทานการสึกหรอได้ดีกว่าชิ้นงานที่ขึ้นรูปโดยการหล่อ แต่มีแนวโน้มที่จะน้อยกว่าการต้านทานการสึกหรอของชิ้นงาน SLM

คำหลัก: การหลอมซ้ำด้วยเลเซอร์, กระบวนการหลอมโดยแสงเลเซอร์, โลหะผสมโคบอล โครเมียม, การพัฒนาคุณภาพผิว, การพิมพ์สามมิติโลหะ

Abstract

Project Code: MRG5980217

Project Title: Surface Improvement of Selective Laser Molten Cobalt

Chromium Alloy by Laser Re-Melting Technique

Investigator: Dr. Supamard Sujatanond
E-mail Address: ssupamar@engr.tu.ac.th
Project Period: 2 May 2016 to 1 May 2018

In order to improve the surface quality of selective laser molten (SLM) Cobalt Chromium (CoCr) alloy, a laser re-melting (LRM) process was applied on the top surface of SLM specimens. The effect of scanning direction, laser processing parameters and scanning number of LRM process on the surface quality of SLM specimens were examined in this study. According to the experimental results, the direction of LRM process in the cross direction to the SLM direction performed as the best condition to reduce the surface roughness. Furthermore, LRM process proved to reduce the surface roughness of SLM specimen. Laser re-melting power (PLRM) is recommended to be equal or more than the laser power used for SLM (P_{SLM}) and laser re-melting scanning speed (V_{LRM}) should be as same as the scanning speed of SLM (V_{SLM}). In addition, the surface roughness can be reduced by increasing the laser remelting power (P_{LRM}) and the repeated number of LRM process. It was found that the LRM condition at P_{LRM}=150W and V_{LRM}=1000 mm/s could reduce the surface roughness of SLM specimen by 45% from about 21.99 to 11.98 µm. Repeating LRM process for 3 times, the surface roughness reduced by 70% from 21.99 to 6.49 µm. However, LRM process resulted in the reduction of specimen's height by approximately 10 µm. Nevertheless, this dimension error can be later added to compensate the dimension of 3D model before printing the part. In addition, the LRM layer was observed to be very thin layer which had a thickness within 200 µm. There is an evidence that there was a decrease of hardness within the LRM layer. The hardness of LRM layer was lower than SLM specimen and higher than that of a commercial casted specimen. Therefore, the change of hardness could affect to the wear behavior of CoCr alloy. Then, the ball-on-disk wear tests were conducted to compare the wear resistance between SLM CoCr alloy and a commercial casted CoCr alloy (With technical problem, LRM wear specimen was unable to fabricate). SLM CoCr alloy showed better wear resistance comparing with a commercial casted CoCr alloy. This agrees with the result of the hardness value which SLM CoCr alloy show higher in hardness compared with casted CoCr alloy.

Keywords: Laser re-melting, Selective laser melting, Cobalt chromium alloys, Surface improvement, Metal 3D Printing

Executive Summary

Nowadays, innovation save lives and improve the quality of the health care. Metal 3D printing, also known as selective laser melting (SLM) process, is one of emerging technology, which could change the world of medical device manufacturing in the years to come. This technology empowers doctors, engineers and medical device manufacturers to work faster to create personalized products from a 3D computer-aided design (CAD) models based on digital images from non-invasive patient diagnostic scans. With SLM technology, medical devices and medical implants can be made to exacting specification in an accurate size and shape with very tight tolerances to ensure an optimal fit inside the patient. However, the surface quality of SLM printed part is relatively poor. The post processes for surface finishing are required such as using CNC machine which results in higher production time and cost. Moreover, dimension error can be occurred during setup sample in CNC machine causing inaccurate size and shape of products.

Laser re-melting (LRM) process is a surface modification technique which can be used to solve the problem of surface finishing. LRM process uses a laser in SLM machine to remelt the surface of SLM printed parts to be smoother surface. There is no need to remove sample out of machine to complete surface finishing. This leads to the elimination of dimension error problem and the reduction of production time while the LRM fabrication time is very fast. So, we are able to build and surface finish a metal parts in only one machine.

LRM process does not only help to improve the surface roughness of materials but it can be used to modify surface properties as well. The microstructures and mechanical properties can be altered depending on the heat induced by LRM process. If we adjust proper LRM processing parameters. We can obtain both roughness and desired properties. For this reason, LRM process can be embedded as a one function in SLM machine without paying additional cost. This technique can be applied to any metals and any kinds of applications. The results from this research already proved the advantage after applying LRM process on the surface of SLM sample. The roughness of SLM part can be reduced up to 70% in this research. The further study of LRM behavior will be continuous to improve the better performance of LRM process for metal 3D printing.

Contents

1.	Introduction.	1
2.	Objective	1
3.	Methodology	1
4.	Results and discussion	4
5.	Conclusion. 4	0
6.	Acknowledgement4	2
7.	References	3
8.	Outcome	4

บทคัดย่อ

รหัสโครงการ: MRG5980217

ชื่อโครงการ: การพัฒนาคุณภาพผิวของโลหะผสมโคบอลต์โครเมียมที่ขึ้นรูปโดยกระบวน

การหลอมโดยแสงเลเซอร์ด้วยเทคนิคการฉายแสงเลเซอร์ซ้ำ

ชื่อนักวิจัย: อาจารย์ คร.สุภมาศ สุชาตานนท์

E-mail Address: ssupamar@engr.tu.ac.th

ระยะเวลาโครงการ: 2 พฤษภาคม 2559 ถึง 1 พฤษภาคม 2561

งานวิจัยนี้ ได้มีการนำกระบวนการหลอมซ้ำด้วยเลเซอร์ (Laser re-melting; LRM) มาใช้เพื่อ พัฒนาคุณภาพผิวของ โลหะผสม โคบอลต์ โครเมียมที่ขึ้นรูป โคยกระบวนการหลอม โคยแสงเลเซอร์ (selective laser melting: SLM) โดยมีการปรับปัจจัยของทิศทางการหลอมซ้ำ ปัจจัยของเลเซอร์ และ จำนวนการหลอมซ้ำที่ส่งผลต่อความเรียบผิวของชิ้นงาน SLM ซึ่งจากผลการทคลองในงานวิจัยนี้ได้ พบว่าการหลอมซ้ำนั้นสามารถช่วยให้ลดความหยาบผิวของชิ้นงาน SLM ได้ โดยทิศทางช่วยลด ความหยาบผิวได้ดีที่สุดนั้นคือทิศทางที่ตั้งฉากกับทิศทางของ SLM และนอกจากนี้ยังพบว่ากำลัง ของเลเซอร์สำหรับการหลอมซ้ำ (Laser re-melting power; P_{LRM}) นั้นควรจะมากกว่าหรือเท่ากับ กำลังที่ใช้ขึ้นรูปชิ้นงาน SLM (P_{SLM}) และความเร็วสำหรับการหลอมซ้ำ (laser re-melting scanning speed; V_{LRM}) ควรเท่ากับความเร็วที่ใช้ขึ้นรูปชิ้นงาน SLM (V_{SLM}) การลดความหยาบผิวให้น้อยลง สามารถทำได้โดยการเพิ่มกำลังของเลเซอร์สำหรับการหลอมซ้ำ ($P_{
m LRM}$) หรือ เพิ่มจำนวนของการ หลอมซ้ำให้มากขึ้น ในการทคลองหลอมซ้ำที่กำลังของเลเซอร์สำหรับการหลอมซ้ำเท่ากับ 150W และความเร็วสำหรับการหลอมซ้ำเท่ากับ 1000 mm/s ได้พบว่าสามารถลดความหยาบผิวของชิ้นงาน SLM ได้จาก 21.99 µm เหลือเพียง 11.98 µm ซึ่งคิดเท่ากับการลดลง 45% ซึ่งถ้าหากทำการหลอมซ้ำ เช่นนี้ซ้ำเป็นจำนวน 3 ครั้งจะทำให้ความหยาบผิวลดลงไปเหลือเพียง 6.49 um ซึ่งเทียบเท่ากับการ ลดลง 70% เมื่อเทียบกับผิวของชิ้นงาน SLM แต่อย่างไรก็ตามกระบวนการหลอมซ้ำด้วยแสงเลเซอร์ ้นั้นจะส่งผลให้ความสูงของชิ้นงานลดลงประมาณ 10 µm แต่อย่างไรก็ตามส่วนต่างนี้สามารถนำไป ้ปรับแต่งในแบบจำนวนก่อนการผลิตชิ้นงานด้วย SLM ภายหลังได้ นอกจากนี้ได้มีการผ่าชิ้นงาน เพื่อศึกษาชั้นผิวของการหลอมซ้ำและได้พบว่าชั้นผิวนี้มีความบางอยู่ที่ต่ำกว่า 200 µm เท่านั้น แต่ อย่างไรก็ตามได้พบว่าค่าความแข็งของชั้นผิวนี้ต่ำกว่าค่าความแข็งของ SLM แต่ยังคงมากกว่าค่า ความแข็งของโลหะผสมโคบอลโครเมียมที่ทำจากการหล่อที่มีขายเชิงพานิชทั่วไป แต่ค่าความแข็ง ของชิ้นงาน LRM ที่แตกต่างไปนั้นอาจส่งผลต่อความสามารถในการต้านทานการสึกหรอได้ ดังนั้น ในงานวิจัยนี้ ใค้มีการศึกษาคณสมบัติการต้านทานการสึกหรอค้วยวิธีบอลออนดิสก์ (ball-on-disk wear test) ของโลหะผสมโคบอลโครเมียมที่ขึ้นรูปโดยการหล่อและวิธี SLM เพื่อเปรียบเทียบกับ ชิ้นงานที่หลอมซ้ำ แต่อย่างไรก็ตามงานวิจัยนี้ไม่สามารถขึ้นรูปชิ้นงานทคสอบการสึกหรอที่ผ่าน การหลอมซ้ำได้ จึงได้ทำการทคสอบเพียงชิ้นงานที่ขึ้นรูปด้วยการหล่อและ SLM ผลการทคลอง พบว่าการต้านทานการสึกหรอของชิ้นงาน SLM นั้นสูงกว่าชิ้นงานที่ทำจากการหล่อ ซึ่งผลนี้ก็ สัมพันธ์กับผลของค่าทคสอบความแข็ง ซึ่งสามารถพยากรณ์ได้ว่าค่าความต้านทานการสึกหรอของ ชิ้นงานที่ผ่านการหลอมซ้ำนั้นอาจมีการต้านทานการสึกหรอได้ดีกว่าชิ้นงานที่ขึ้นรูปโดยการหล่อ แต่มีแนวโน้มที่จะน้อยกว่าการต้านทานการสึกหรอของชิ้นงาน SLM

คำหลัก: การหลอมซ้ำด้วยเลเซอร์, กระบวนการหลอมโดยแสงเลเซอร์, โลหะผสมโคบอล โครเมียม, การพัฒนาคุณภาพผิว, การพิมพ์สามมิติโลหะ

Abstract

Project Code: MRG5980217

Project Title: Surface Improvement of Selective Laser Molten Cobalt

Chromium Alloy by Laser Re-Melting Technique

Investigator: Dr. Supamard Sujatanond
E-mail Address: ssupamar@engr.tu.ac.th
Project Period: 2 May 2016 to 1 May 2018

In order to improve the surface quality of selective laser molten (SLM) Cobalt Chromium (CoCr) alloy, a laser re-melting (LRM) process was applied on the top surface of SLM specimens. The effect of scanning direction, laser processing parameters and scanning number of LRM process on the surface quality of SLM specimens were examined in this study. According to the experimental results, the direction of LRM process in the cross direction to the SLM direction performed as the best condition to reduce the surface roughness. Furthermore, LRM process proved to reduce the surface roughness of SLM specimen. Laser re-melting power (P_{LRM}) is recommended to be equal or more than the laser power used for SLM (P_{SLM}) and laser re-melting scanning speed (V_{LRM}) should be as same as the scanning speed of SLM (V_{SLM}). In addition, the surface roughness can be reduced by increasing the laser remelting power (P_{LRM}) and the repeated number of LRM process. It was found that the LRM condition at P_{LRM}=150W and V_{LRM}=1000 mm/s could reduce the surface roughness of SLM specimen by 45% from about 21.99 to 11.98 µm. Repeating LRM process for 3 times, the surface roughness reduced by 70% from 21.99 to 6.49 µm. However, LRM process resulted in the reduction of specimen's height by approximately 10 µm. Nevertheless, this dimension error can be later added to compensate the dimension of 3D model before printing the part. In addition, the LRM layer was observed to be very thin layer which had a thickness within 200 µm. There is an evidence that there was a decrease of hardness within the LRM layer. The hardness of LRM layer was lower than SLM specimen and higher than that of a commercial casted specimen. Therefore, the change of hardness could affect to the wear behavior of CoCr alloy. Then, the ball-on-disk wear tests were conducted to compare the wear resistance between SLM CoCr alloy and a commercial casted CoCr alloy (With technical problem, LRM wear specimen was unable to fabricate). SLM CoCr alloy showed better wear resistance comparing with a commercial casted CoCr alloy. This agrees with the result of the hardness value which SLM CoCr alloy show higher in hardness compared with casted CoCr alloy.

Keywords: Laser re-melting, Selective laser melting, Cobalt chromium alloys, Surface improvement, Metal 3D Printing

"Surface Improvement of Selective Laser Molten Cobalt Chromium Alloy by Laser Re-Melting Technique"

1. Introduction

Selective Laser Melting (SLM) process is one of the additive manufacturing processes that fabricates three-dimensional metal parts using laser to fully melt metal powder layer by layer [1,2]. SLM process can create complex geometry and individualized components, therefore it is suitable for medical and dental applications, for example, femoral head for a total hip replacement as shown in Fig.1 [3]. Cobalt Chromium (CoCr) alloys are commonly used for femoral head because of their good combination of mechanical strength and ductility [4]. In practical, surface smoothness reduces over time accelerating wear in liner's surface which leads to failure of components. Therefore, it is important

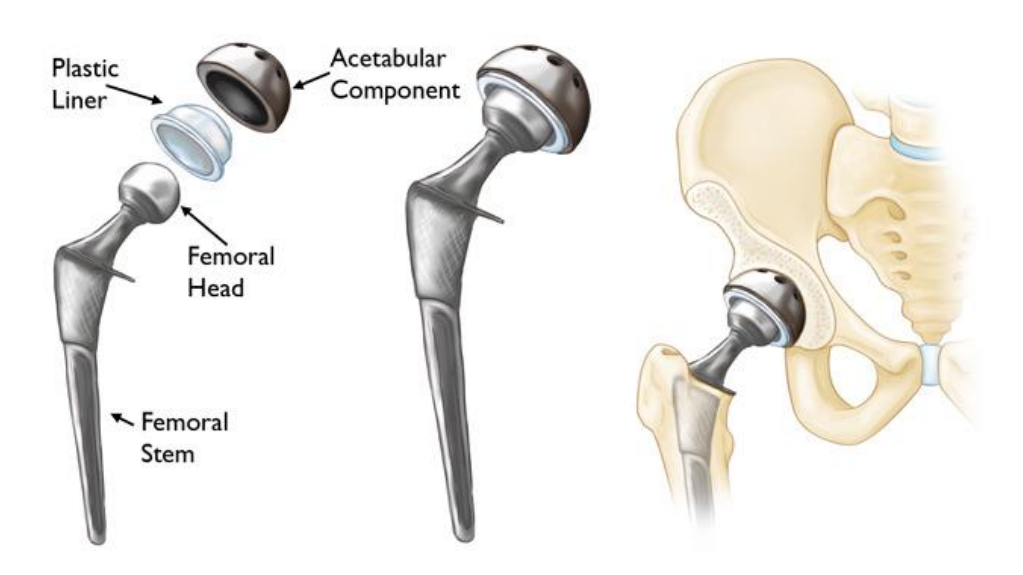


Fig.1 Components for total hip replacement [3].

to improve surface roughness and hardness of SLM part's surface without decreasing desired ductility of the substrate.

In order to improve the surface roughness of SLM parts, the conventional machining processes are required as a post process to make a smoother surface, for example CNC milling, resulting in the increase of production time. Therefore, it is a challenge to improve surface quality of SLM without using other post processes. In general, processing parameters such as laser power, scanning speed, laser defocus and hatch spacing are varied to find the suitable conditions to reduce the surface roughness. However, the surface roughness of SLM is still poor to apply into medical applications [5].

Laser re-melting is a surface modification technique which generally used after the conventional-manufacturing processes to re-melt surface of materials to improve surface quality such as hardness, wear resistance, corrosion resistance, wettability and roughness. Principle of laser re-melting is shown in Fig.2 [6]. Heat energy generated by laser beam is applied on the rough surface to re-melt uneven area, then the molten area will be solidify to be a smoother surface

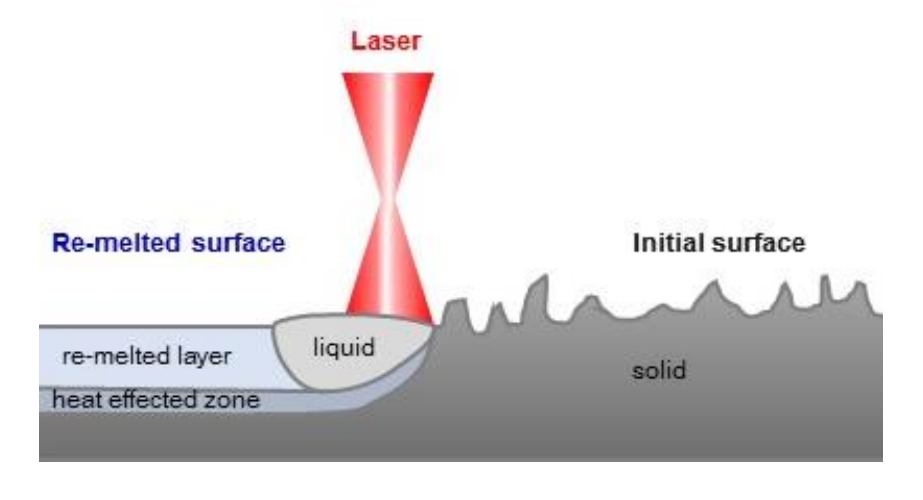


Fig.2 Laser re-melting process.

as illustrated in Fig.2. Therefore, it is interesting to introduce this technique to SLM parts to improve the surface quality after SLM process without using other conventional manufacturing processes. In some research works also apply laser re-melting in every layers during SLM process. This could lead to reducing in porosity and increasing in the density of each layers of SLM parts which could enhance the mechanical strength and the fatigue life [7].

E. Yasa et al. applied a laser re-melting process on each layer of 316L stainless steel powders during SLM process, it was found that laser re-melting results in the reduction of the porosity in inner density and shell density of SLM part [7,8]. Moreover, the surface roughness found to be varied depending on the inclination angle of surface at the same laser re-melting condition. After apply laser re-melting on the variety of inclined surface, it is clear that the roughness increased with increasing in the inclination angle of surface. The results also showed that the laser re-melting can reduced the roughness by 10-15% compared with as-fabricated SLM part. Moreover, Costel-Relu Ciubotariu et al. reveals that the number of re-melting scan can enhance the surface quality of Stellite 6 coating layer on martensite stainless steel type 1.4313 [9].

To improve the wear resistance, nitrogen-ion implantation is an alternative to improve surface hardness of CoCr alloy by diffusing a nitrogen ion into substrate's surface to form a thin ceramic nitride film on surface to enhance wear resistance and to reduce friction [10]. Furthermore, there is a report that using laser re-melting to improve hardness and wear resistance of materials. Laser re-melting generates the heat to induce the microstructural and phase modifications which can improve the hardness in the re-melting zone of steel [11].

For this reason, this research aims to improve the surface quality of SLM parts by using a laser re-melting technique on the surface of SLM parts. With the high energy laser beam, it is able to melt a rough surface of SLM parts and solidify to smoother surface. Moreover, the microstructures and properties of material's surface can modified depending on the LRM processing parameters. Furthermore, the laser re-melting will be conducted in the nitrogen environment in order to form a thin nitride layer on the surface to increase the hardness and the wear resistance.

2. Objective

This research aims to introduce a laser re-melting (LRM) technique to improve surface quality of CoCr alloy after the selective laser melting (SLM) process in the N₂ environment. Moreover, surface roughness, mechanical properties and wear resistance of LRM specimens were also investigated in this study. Furthermore, the dimension change due to LRM process were also clarify in this work

3. Methodology

This research works divided into three main experiments. Firstly, the effect of scanning direction, laser power and scanning speed of the laser remelting (LRM) process were studied. In the next step, the effect of scanning number of laser re-melting were examined in order to improve surface quality.

Finally, preliminary study of wear behavior of CoCr alloy were carried out in this study.

3.1 Scanning direction, laser power and scanning speed tests

Cobalt-Chromium (Co-Cr) alloy ASTM F75 powders are used in this research. The chemical compositions are shown in Table 1. CoCr alloy powders are in spherical shape as shown in Fig.3. The particle size distribution are ranged from 20 to 45 µm with the average particle size of 36 µm as shown in Table 2. Self-developed SLM machine manufactured by the National Metal and Materials Technology Center (MTEC) were used in this experiments as shown in Fig.4. This machine is equipped with the continuous wave (CW) fiber laser with the wavelength of 1064 nm. The maximum power input is 300W. The laser spot size is approximately 80 µm. In the experiments, SLM specimens were fabricated into the size of 10×10×5 mm³ as shown in Fig.5. SLM specimens were printed on the SS400 steel platform. The experimental conditions were summarized in Table 3.

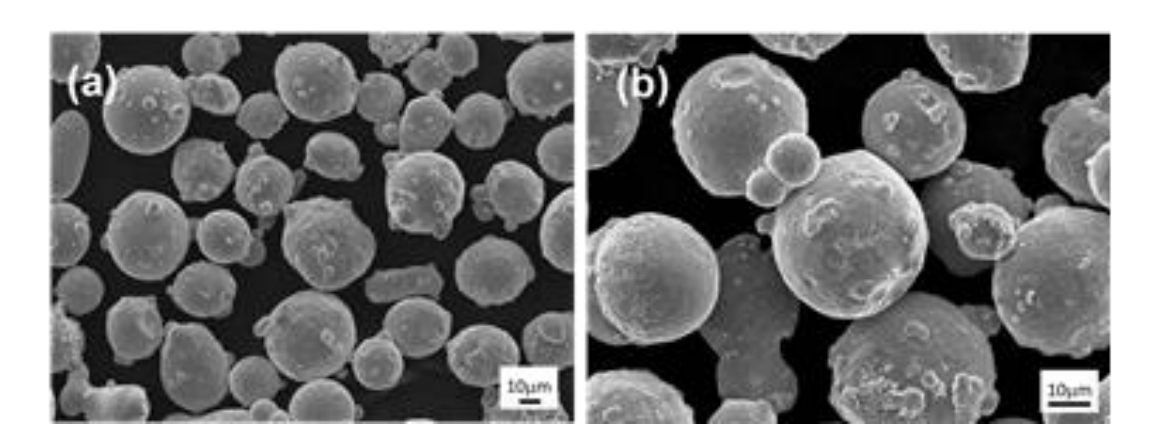


Fig.3 CoCr alloy powder particles morphology (a) 500× Magnification and (b) 1000× Magnification.

Table 1 The chemical compositions of Cobalt-Chromium (Co-Cr) alloy ASTM F75.

Element	%	Element	%	Element	%
Cr	28.7%	K	0.27%	N	0.16%
Mo	5.8%	La	0.27%	Ni	0.16%
Ge	1.36%	Na	0.27%	Sr	0.14%
In	1.36%	Pb	0.27%	Н	0.13%
Nb	1.36%	Sn	0.27%	О	0.016%
Se	1.36%	Te	0.27%	W	0.012%
T1	1.36%	Zn	0.27%	P	0.009%
V	1.36%	Zr	0.27%	S	0.004%
Si	0.68%	С	0.19%	Ti	0.002%
Mn	0.56%	Fe	0.16%	Co	Balance

Table 2 The particle size distribution.

Size (µm)	%
>45	1.6
20 <size<45< th=""><th>94.1</th></size<45<>	94.1
<20	4.3

Table 3 Experimental conditions

Duo aggain a		LRM		
Processing parameters	SLM	Scanning direction test	P _{LRM} and V _{LRM} tests	
Laser power (P)	100 W	50, 100, 150 W	50, 75, 100, 125, 150 W	
Scanning speed (v)	1,000 mm/s	1,000 mm/s	500, 1000, 1500 mm/s	
Hatch spacing (H)	180 µm	180 μm	180 µm	
Layer thickness (t)	100 µm	-	-	
Environment	N ₂	N_2	N ₂	
Direction of LRM	-	0°, 45°, 90°	90°	

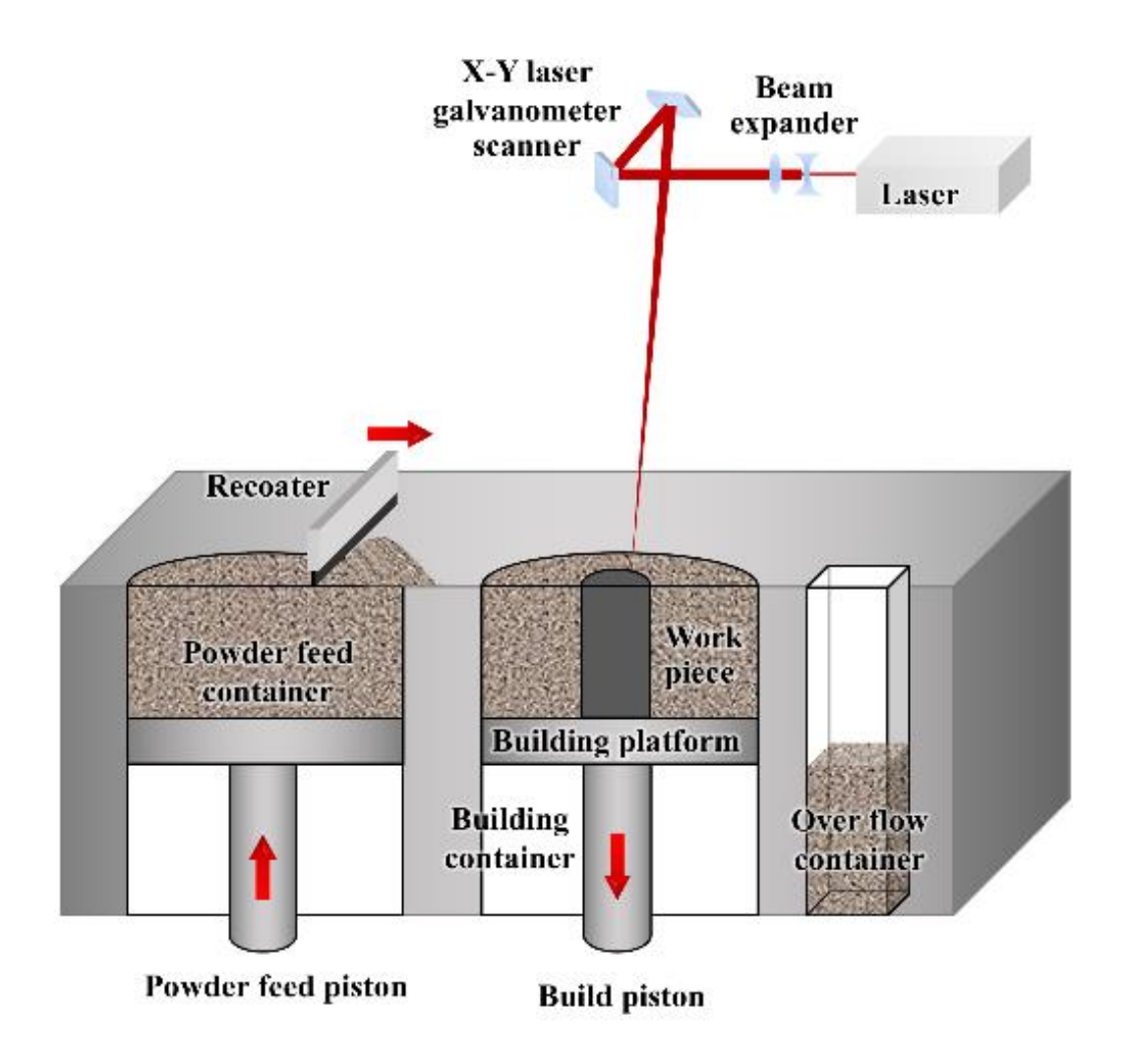


Fig.4 SLM and LRM processes.

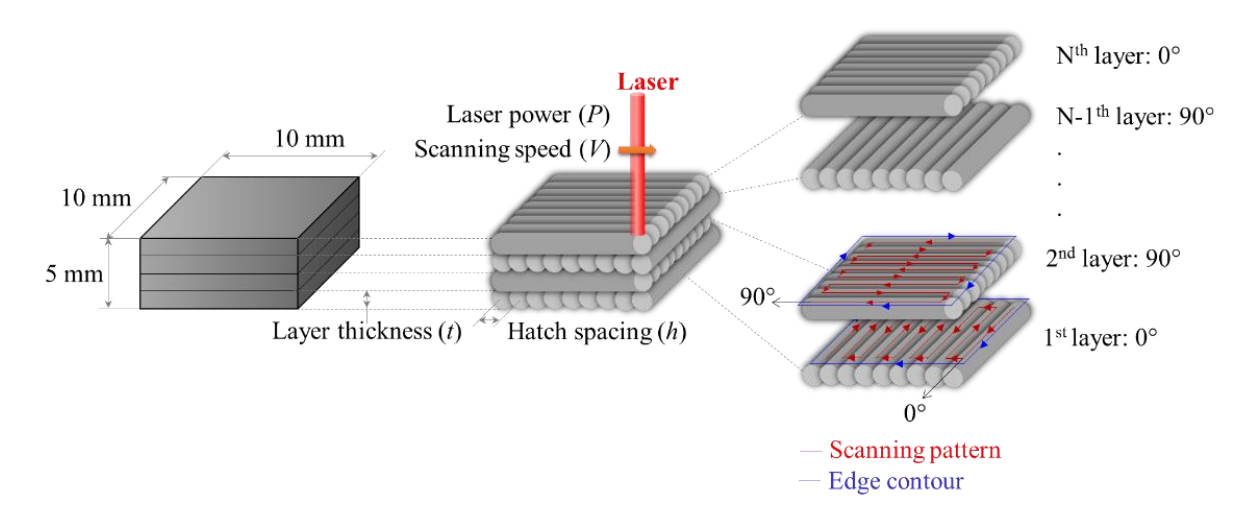


Fig.5 SLM Specimen.

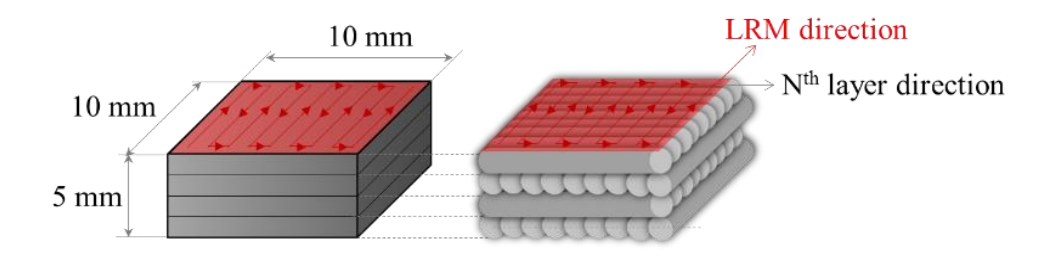


Fig.6 LRM specimen.

Laser power (P_{SLM}) and scanning speed (V_{SLM}) were 100 W and 1000 mm/s, respectively. Moreover, the 99.99% of N₂ was supplied in the SLM machine's chamber to prevent specimens from the oxidation. In SLM process, powders layer of 100 µm thickness (t) were selectively melted to into a single line and each single lines were connected with the hatch spacing (h) of 180 µm following by edge contouring as shown in Fig.5. Then, the next layer were built on the top of the previous layer in the cross direction (90°) to previous layer. After the fabrication of SLM specimen, laser re-melting (LRM) process was applied on the top surface of SLM specimen in the scanning direction of 0°, 45° and 90° to Nth layer of SLM in order to find the proper direction for LRM as shown in Fig.6. After obtain the proper direction of LRM scan, laser re-melting power (P_{LRM}) and scanning speed (V_{LRM}) were varied in the next experiments. The parameters were selected to be lower and higher than the laser power (P_{SLM}) of 100 W and the scanning speed (V_{SLM}) of 1000 mm/s. Laser re-melting power (P_{LRM}) were tested at 50, 75, 100, 125 and 150 W. For the scanning speed (V_{LRM}), this parameter were varied at three levels which were 500, 1000 and 1500 mm/s in the experiments. The hatch spacing (h) was fixed at 180 µm during LRM process as shown in Fig.5.

After the tests, the surface observation and material analysis were carried out. Surface appearance was observed by a digital microscope, confocal laser scanning microscope and scanning electron microscope (SEM) to examine the LRM surface. Surface roughness were measured by non-contact method using a confocal laser scanning microscope. Moreover, specimens were cut and ground to observe the macro- and microstructure in the LRM layer. Specimens were etched by the electrolytic etching at E=3V for 3-5 s using the solution of 20 ml of nitric acid (HNO₃) and 60 ml of hydrochloric acid (HCl). In addition, the effect of LRM on the change of dimension were carried out by a coordinate measuring machine (CMM). Hardness were measured using a Rockwell hardness tester and Vickers hardness tester.

3.2 Scanning number test

As LRM process may help to improve the surface quality, then if we repeat this process for several times, there is a possibility that we could improve better surface quality. For this reason, the numbers of LRM scan were varied and examined in this study as well. The numbers of LRM scan (N_{LRM}) were processed from 1-3 times as shown in Fig.7. The experimental conditions are summarized in Table 4.

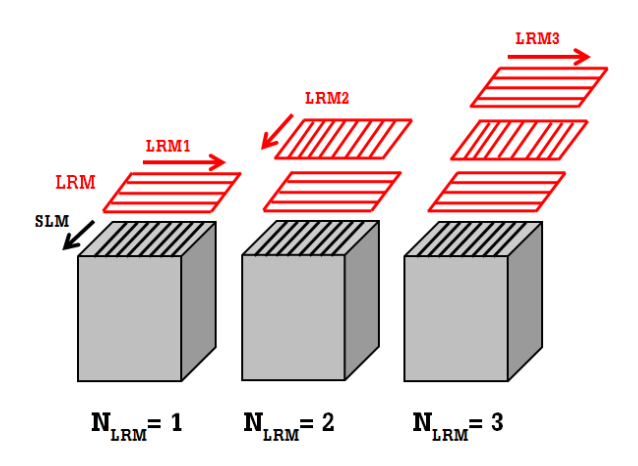


Fig.7 Specimens of the scanning number of laser re-melting test.

Table 4 Experimental conditions for the scanning number of laser re-melting tests

Progagging paramatars	SLM	LRM	
Processing parameters	SLIVI	scanning number test	
Laser power (P)	100 W 50, 100, 150 V		
Scanning speed (v)	1,000 mm/s	1000	
Hatch spacing (H)	180 µm	180 µm	
Layer thickness (t)	100 µm	-	
Environment	N_2	N_2	
Direction of LRM	-	90°	
Number of LRM scan	-	1,2,3	

3.3 Wear tests

Wear tests were conducted to compare the wear resistance of CoCr alloy. Ball-on-disk wear tests were conducted referring to ASTM G133-05 standard test method for linearly reciprocating ball-on-flat sliding wear using an Anton Paar Tribometer as shown in Fig.8. Wear disk made of casted CoCr alloy and SLM



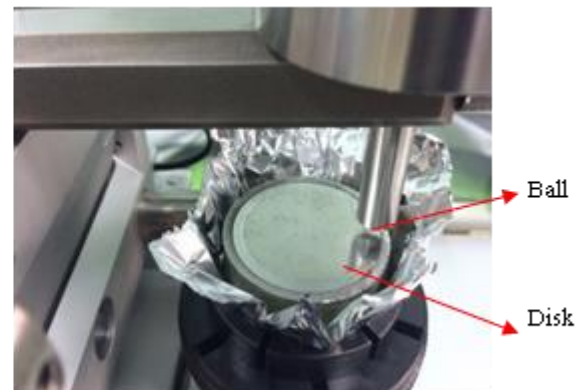


Fig.8 Anton Paar Tribometer.

CoCr alloy. Wear disk was ground until the surface roughness (R_a) was less than 0.8 μ m to meet the requirement of testing standard. However, the surface of LRM disk revealed very poor surface roughness. Once, we polished the top surface to obtain R_a <0.8 μ m, all the LRM layer were polished and removed from specimen. For this reason, the wear tests were conducted only for casted CoCr alloy and SLM CoCr alloy.

Wear disks were fabricated into the diameter of 42 mm and the thickness of 15 mm. SLM disk was fabricated with the laser power (P_{SLM}) of 100 W and scan speed (V_{SLM}) of 1000 mm/s in N_2 environment as shown in Fig.9 and Fig.10.

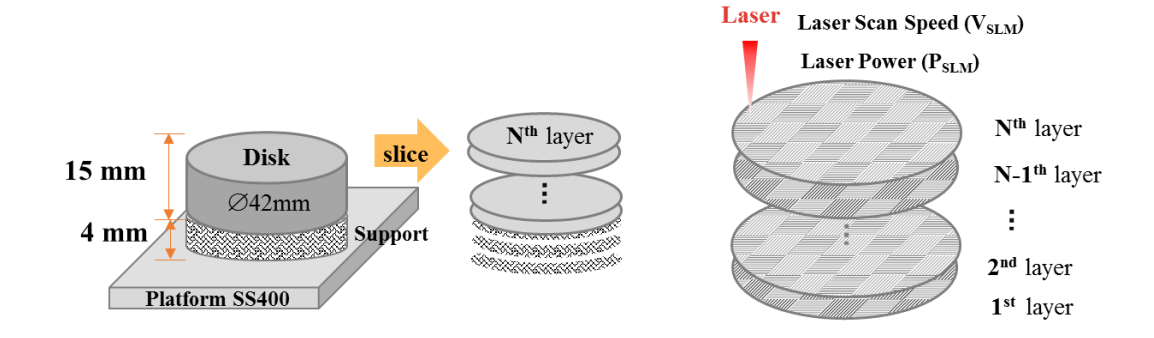


Fig.9 SLM and LRM disks for wear test.



Fig.10 SLM disk.



Fig.11 alumina (Al₂O₃) ball

Scanning strategy was chess board with the hatch spacing (h) of $180 \,\mu m$ and layer thickness (t) of $100 \,\mu m$. In the experiments, alumina (Al₂O₃) ball with the diameter of 6 mm was used as shown in Fig.11. The properties of alumina ball are presented in Table 5. Alumina ball was applied on a CoCr disk at the wear track (R_t) of 18 mm with the load of 10 N as shown in Fig.12. Wear tests were carried out with the sliding speed (V) of 300 mm/s and the sliding distance (d) of 3000 m. Testing conditions were listed in Table 6.

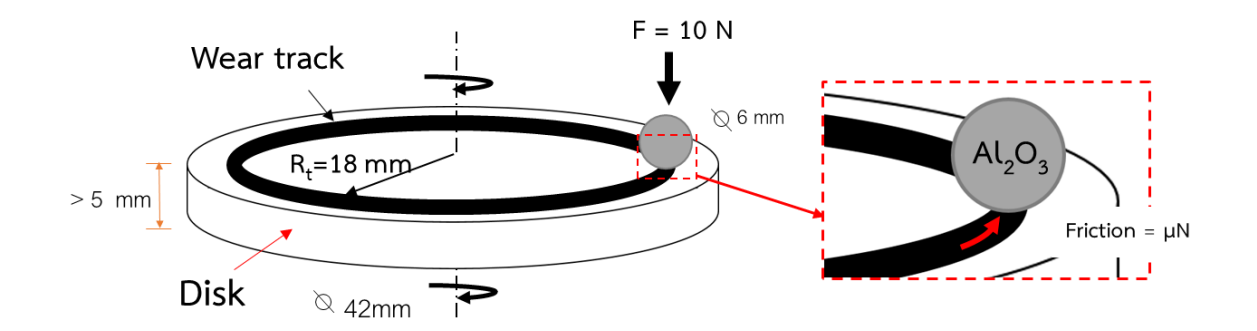


Fig.12 Wear test conditions.

Table 5 The properties of alumina ball

Material	99 % Alumina (Al ₂ O ₃)
Ball diameter	6 mm
Hardness (HRC)	>65
Density	0.0034 g/mm ³

Table 6 Wear test conditions.

Load (F)	10 N
Sliding Speed (V)	300 mm/s
Rotation speed	158.89 rpm
Distance (d)	3000 m
Radius of wear track (Rt)	18 mm
Temperature, Humidity	25°C , 40-55 %RH
Diameter	6 mm
Hardness	>65 HRC
Density	0.0034 g/mm^3
material	Density (ρ)
Ball Alumina	0.0034 g/mm^3
Cobalt Chromium Alloy (Casting)	0.00841 g/mm ³
Cobalt Chromium Alloy (SLM)	0.0083 g/mm ³

4. Results and Discussion

SLM and LRM specimens were built successfully as shown in Fig. 13.

The experimental results are described in the following sections.

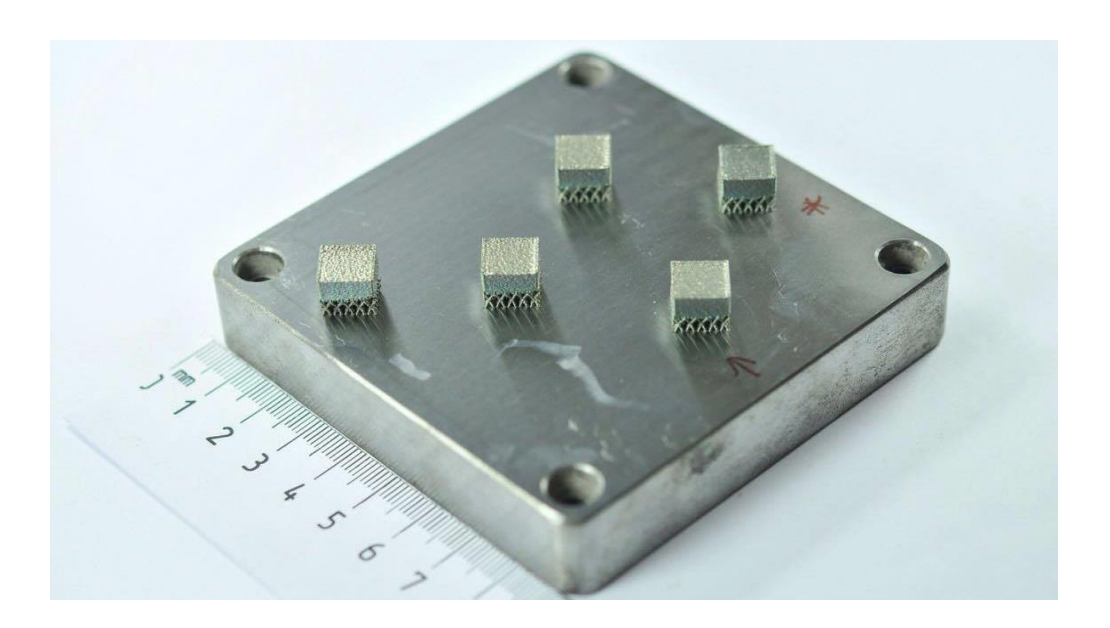


Fig.13 SLM and LRM specimens on the building platform.

4.1 The effect of scanning direction on LRM process

Before conducting LRM tests, SLM specimen was fabricated and measured the surface roughness. The surface roughness were measured in the direction of 0°, 45° and 90° to Nth layer. The average roughness measured on SLM surface are shown in Fig.13. It can be seen that the average roughness values show the highest number in the 90° direction to Nth layer. Therefore, the roughness measured in the cross direction to fabrication direction shows the critical roughness value in the specimen. If we can improve the critical roughness value to be lower, then the overall roughness of specimen may reduce. Thus,

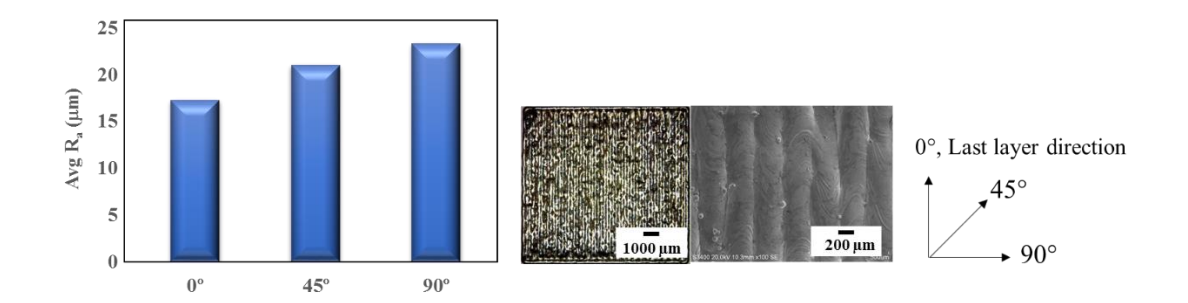


Fig.13 Average roughness of SLM specimens (P_{SLM} =100 W, V_{SLM} =1000 mm/s) measured in 0°,45°,90° to N^{th} layer.

Table 7 The surface observation of LRM specimens in the different scanning direction by using digital microscope.

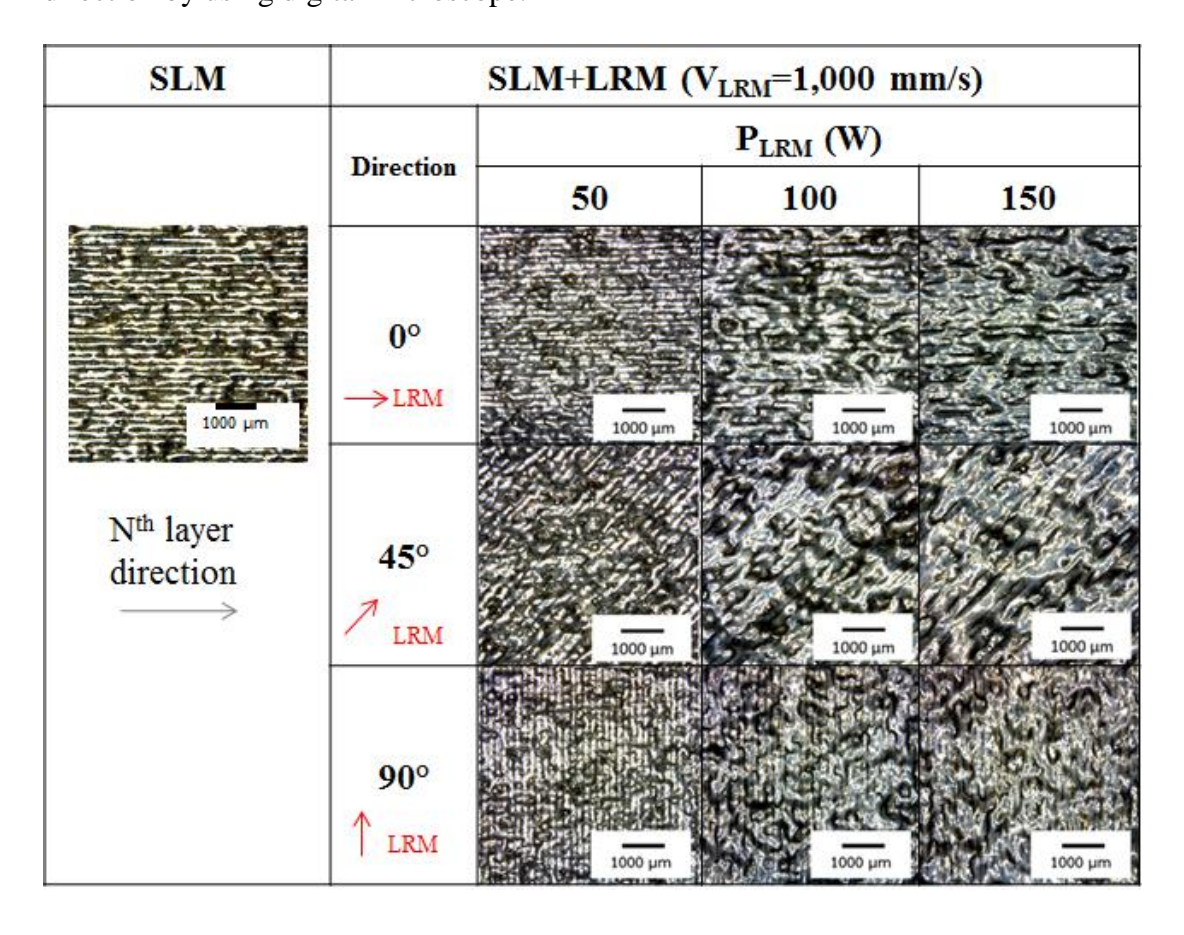


Table 8 The surface observation of LRM specimens in the different scanning direction by using scanning electron microscope (SEM).

SLM	SLM+LRM (V _{LRM} =1,000 mm/s)				
	Direction	P _{LRM} (W)			
	Direction	50	100	150	
16 7mm 1000 002	0° →LRM	27mm.opti0.00 100 µm	лессяко 20 (ку (13-ж ₁₀₀₀ 100 µm	1 1-mm = 100 μm	
N th layer direction	45°	100 µm	100 μm	100 µm	
	↑ 90° LRM	100 µm	100 µm	100 µm	

surface roughness in this research will be measured in the perpendicular direction to the LRM direction to find the critical roughness value in the specimens.

Next, the surface roughness of SLM specimen (P_{SLM} =100 W, V_{SLM} =1000 mm/s) were measured in 90° to the top layer (N^{th} layer) and the average roughness (R_a) was 21.99 μ m. In the next step, the LRM experiments were conducted in the different direction of LRM scan and the results revealed in Table 7 and Table 8.

Then, the surface roughness were measured on the LRM surface layer of every conditions. The measurement of roughness were carried out in the cross direction to the LRM scanning direction as can be seen in Fig.14. The results of

surface roughness are shown in Fig.15. It is obvious that LRM direction in 90° to Nth layer direction shows lower in roughness (R_a) in every level of laser power. For these reason, LRM direction were selected and set at 90° to Nth layer direction in the next experiments.

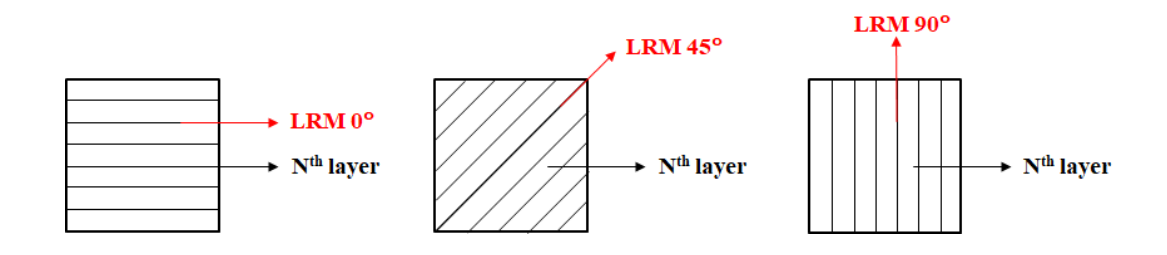


Fig.14 Surface roughness were measured in the cross direction to the LRM direction

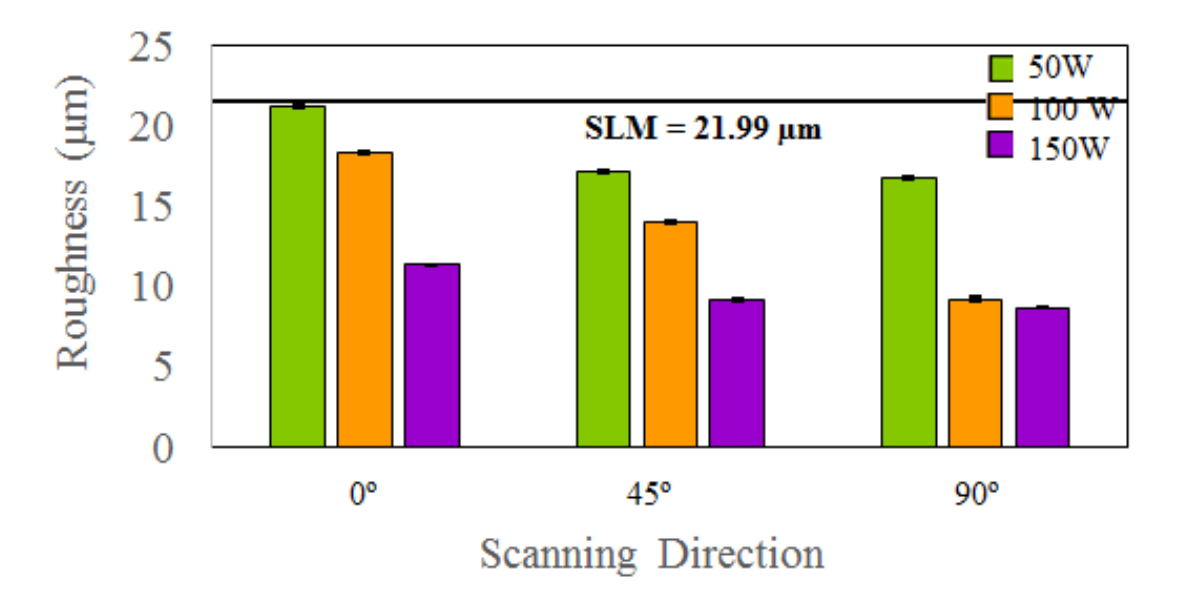


Fig.15 Surface roughness of LRM specimens with the difference of the scanning direction.

4.2 The effect of laser power and scanning speed of LRM process

Laser power (P_{LRM}) and scanning speed (V_{LRM}) of LRM were varied to study the effect of them on the surface quality of SLM specimens. LRM specimens were built successfully in the conditions of the laser re-melting power (P_{LRM}) of 50, 75, 100, 125, 150 W and the scanning speed (V_{LRM}) of 500, 1000, 1500 mm/s. The experimental results are described in the following sections.

4.2.1 Surface and cross-sectional area observation

Surface appearance of laser re-melting (LRM) specimens are shown in Table 9 and Table 10. It can be noticed that LRM surface patterns are classified

Table 9 The surface observation of LRM specimens in the different laser power and scanning speed by using digital microscope.

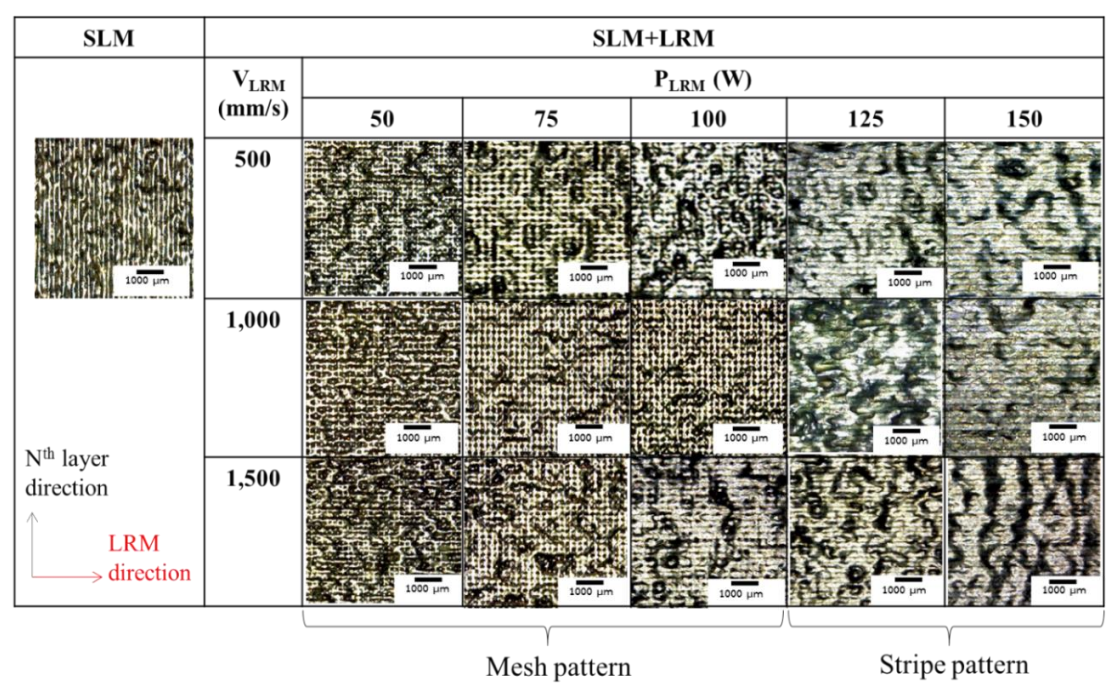
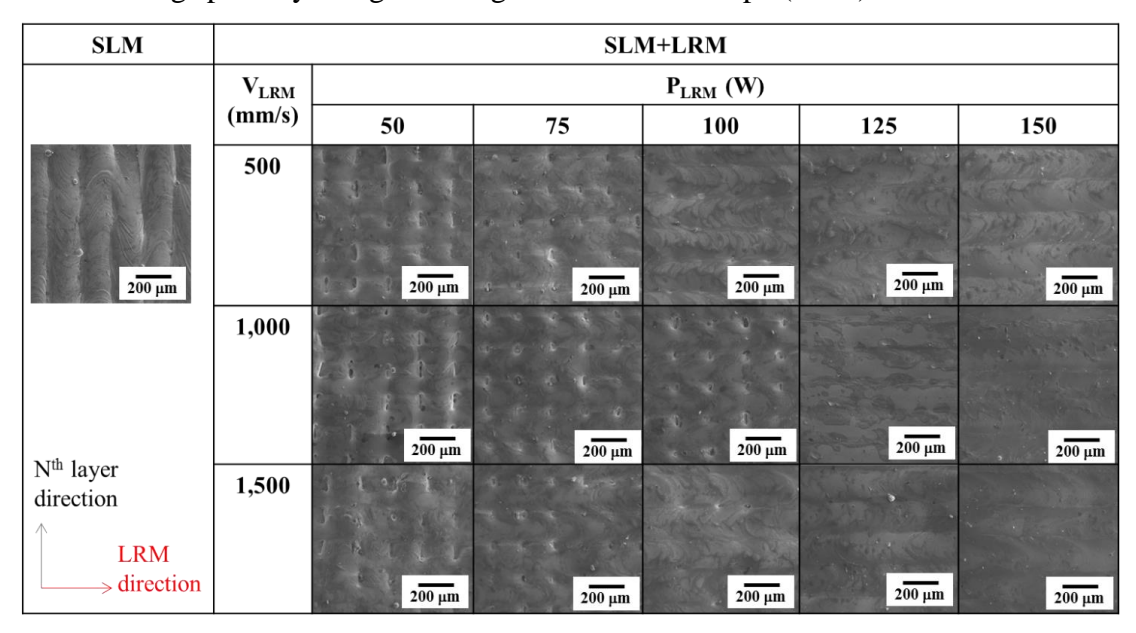


Table 10 The surface observation of LRM specimens in the different laser power and scanning speed by using scanning electron microscope (SEM).



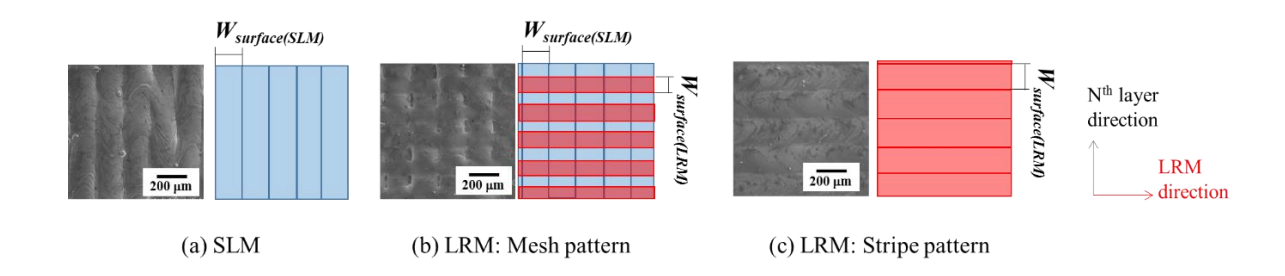


Fig.16 Surface patterns of SLM and LRM specimens.

into two patterns; mesh- and stripe patterns as shown in Fig.16. When the laser remelting power (P_{LRM}) were lower than 100 W, it reveals a mesh-like surface patterns on the LRM surface. The pattern becomes in a stripe-like surface pattern when laser power is over 100 W. The average width of LRM lines ($W_{surface(LRM)}$) were measured on the specimen surface compared with the average of width of SLM line ($W_{surface(SLM)}$) as shown in Fig.17. It is clear that $W_{surface(LRM)}$ are equal and higher than $W_{surface(SLM)}$ when P_{LRM} are higher than 100 W. From these results,

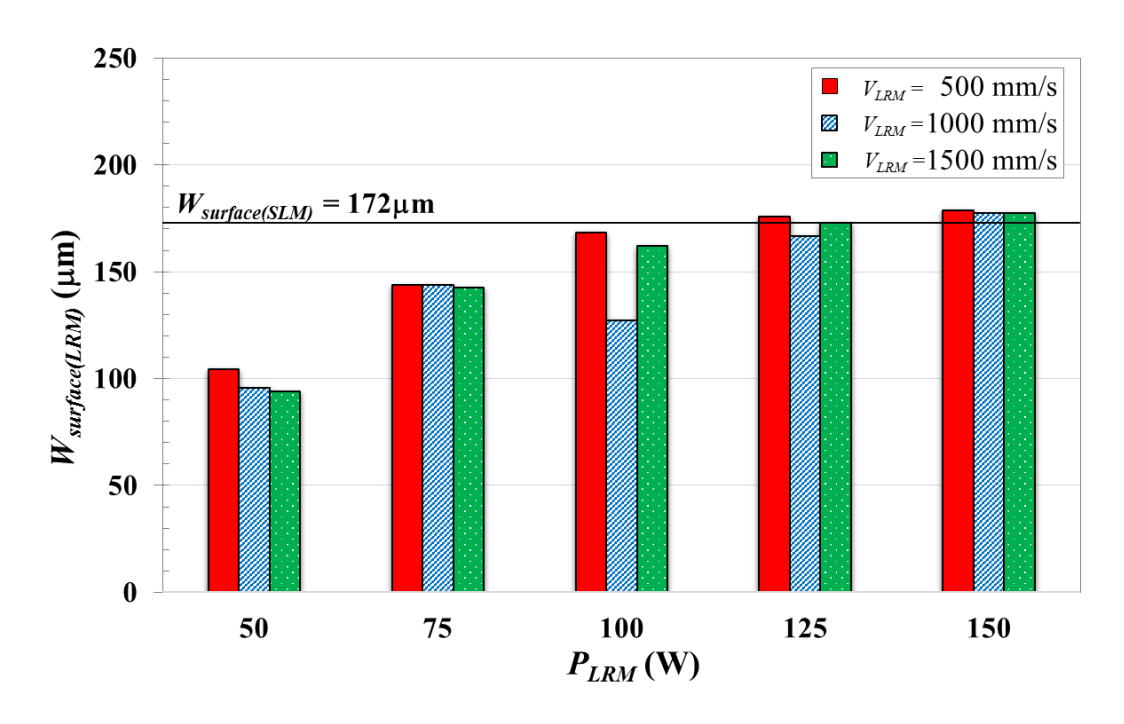
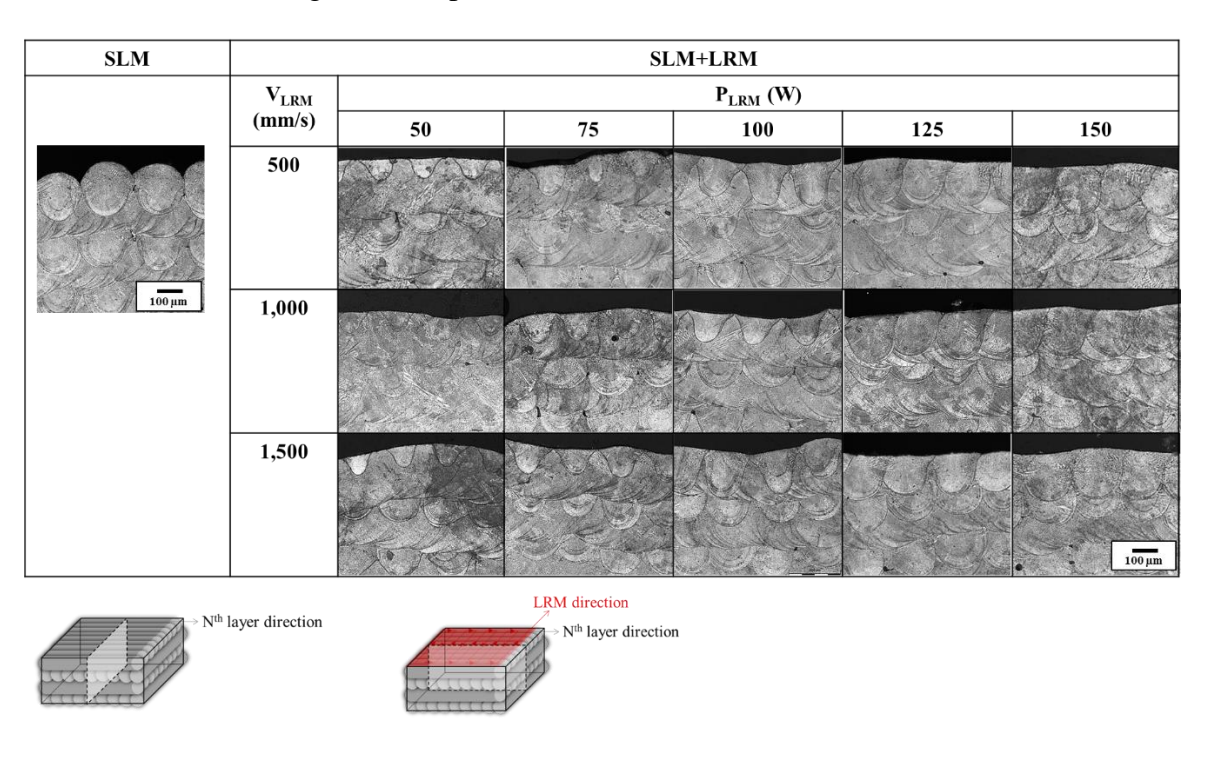


Fig.17 The average width of LRM on the specimen surface $in \ the \ different \ levels \ of \ P_{LRM} \ and \ V_{LRM}.$

Table 11 Cross-sectional section of SLM specimen and LRM specimens using a confocal laser scanning microscope.



it is obvious that the $W_{\text{surface}(LRM)}$ increased with increasing of P_{LRM} and decreasing of V_{LRM}

Moreover, the cross sectional-area of SLM and LRM specimens were observed as shown in Table 11. LRM layer was scanned in the cross direction to the Nth layer of SLM specimen. In each LRM conditions, the width (W_{cross-section(LRM)}) and the laser penetration depth (D_{cross-section(LRM)}) of LRM line in the cross-sectional area (Fig.18) were measured and plotted in the Fig.19 and Fig.20, respectively.

According to Figure 19 and Figure 20, it reveals that the width and depth of LRM layer increased with increasing of P_{LRM} and decreasing of V_{LRM} . The LRM lines became to connect to each other when P_{LRM} is more than 75 W. At lower power, the width was less than the hatch spacing (H) which was 180 μ m. For this reason, there are a discontinuous between each scanning lines resulting in the meshed-like pattern in the LRM layer as shown in Fig.21. For the penetration depth of LRM layers, they were lower than 200 μ m which were less than the depth of the Nth layer of SLM specimen in every conditions. Therefore, there is no effect of LRM inside the core material.

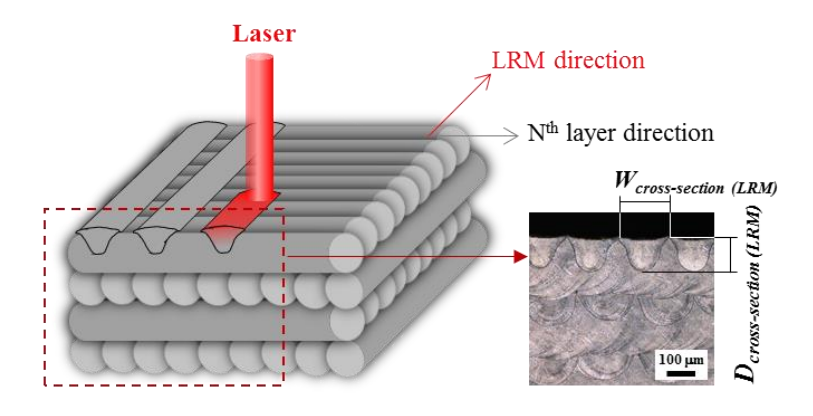


Fig.18 The cross-sectional LRM pattern.

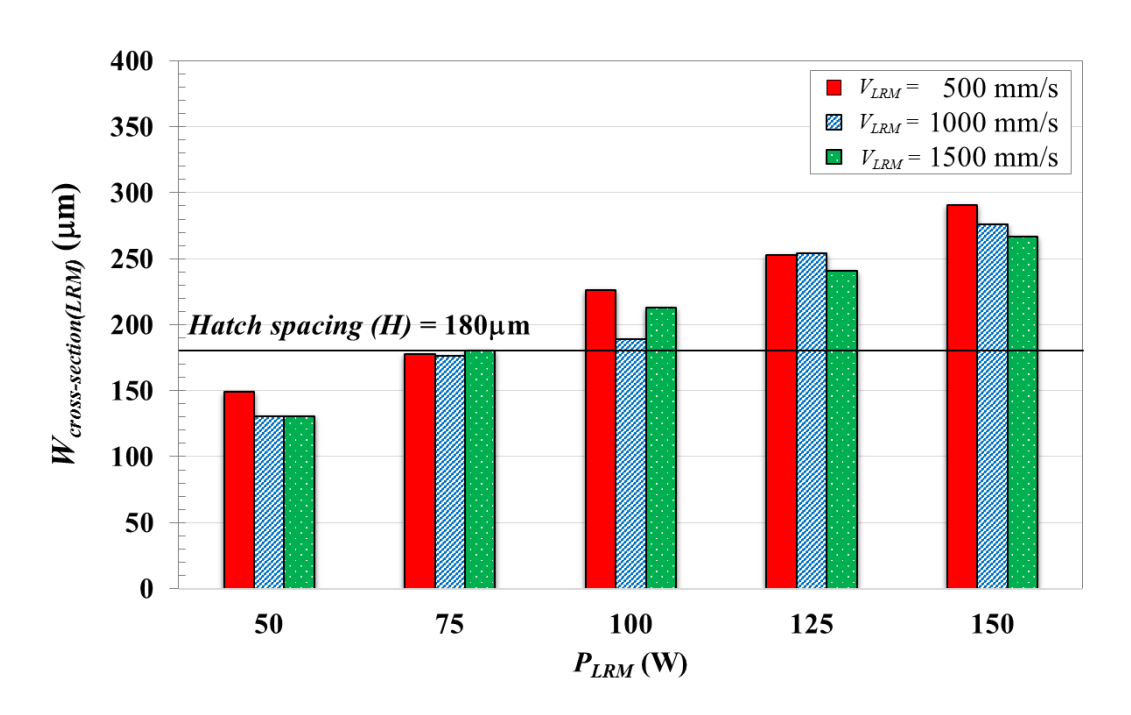


Fig.19 The average width of LRM lines in the cross-sectional area in the different levels of P_{LRM} and V_{LRM} .

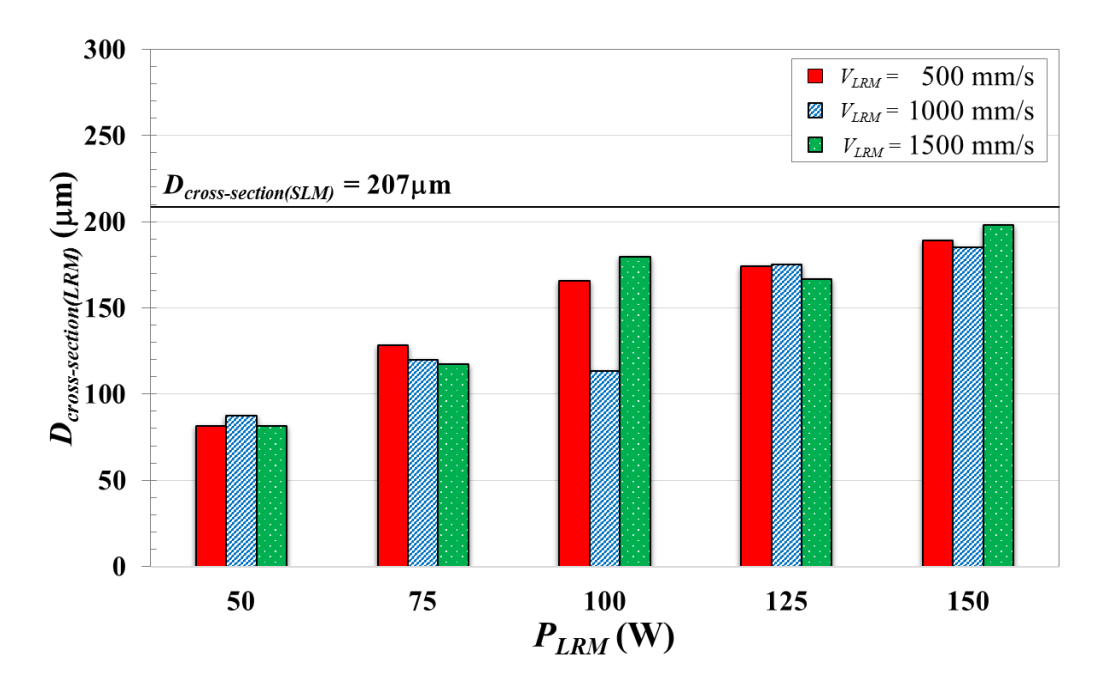


Fig.20 The average penetration depth of LRM lines in the cross-sectional area in the different levels of P_{LRM} and V_{LRM} .

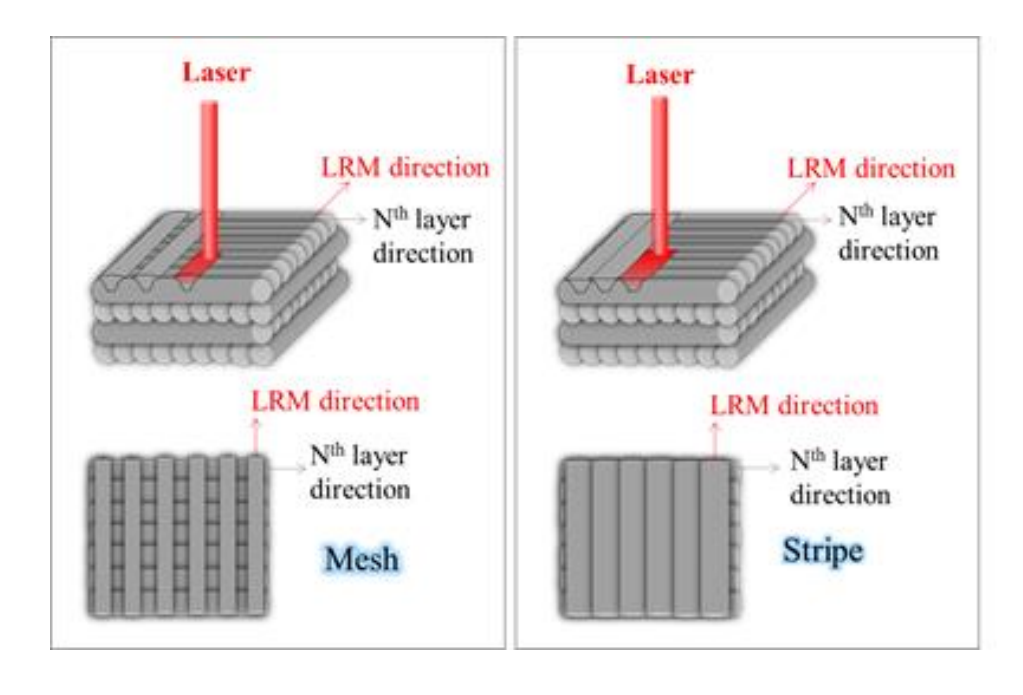


Fig.21 The effect of the width of LRM lines on LRM patterns.

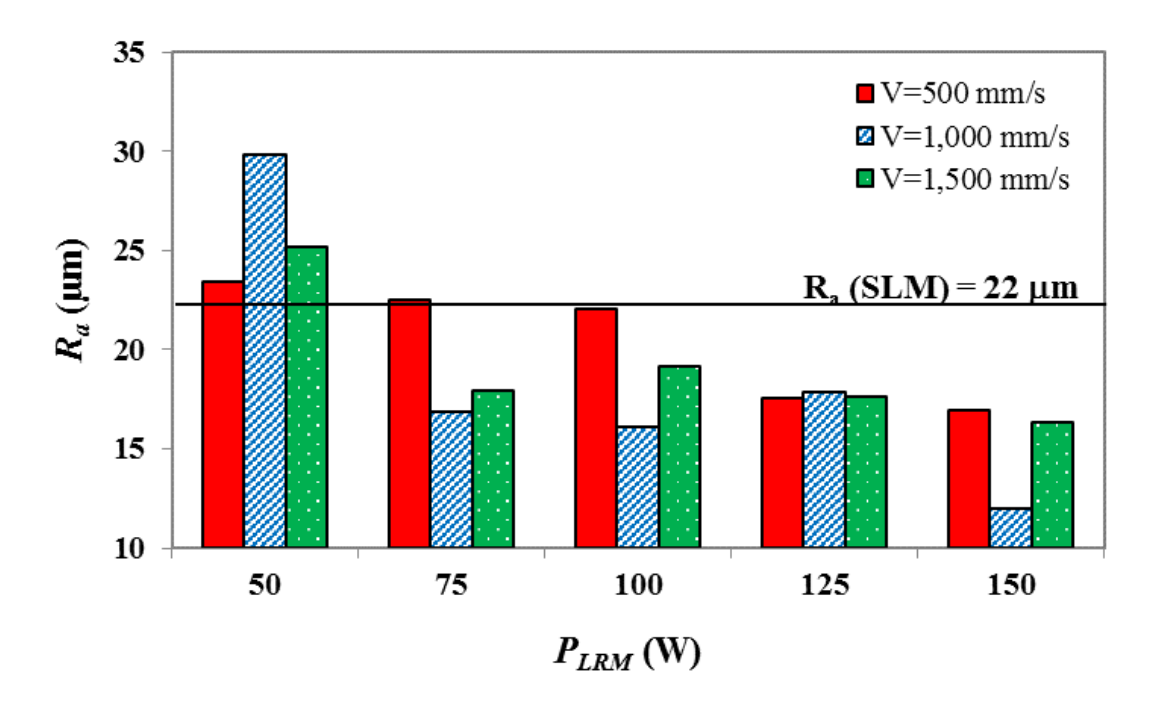


Fig.22 Average roughness (R_a) of LRM specimens measured in the perpendicular direction to N^{th} layer.

4.2.2 Surface roughness

The roughness were measured in the direction of 90° to LRM direction in all cases and summarized in Fig.22. It is clear that laser re-melting process leads to the reduction of surface roughness in all cases except at the condition of $P_{LRM}=50$ W. Surface roughness decreased with increasing P_{LRM} . However, it was found that V_{LRM} at 1000 mm/s (equal to V_{SLM}) shows better surface roughness compared with other levels of V_{LRM} . According to the results, the surface could reduce by 45% after applying LRM process. The lowest surface roughness which could obtain in this experiment was about $11.976~\mu m$ from the experimental condition of $P_{LRM}=150$ W and $V_{LRM}=1000$ mm/s.

4.2.2 Hardness

Macro-hardness tests were conducted using a Rockwell scale C hardness tester on the top surface of SLM and LRM specimens and the results are shown in Fig.23. It can be seen that LRM leads to the decline of hardness value when compared with SLM specimen (47.77 HRC). In addition, the hardness value of LRM specimens become close to the commercial casted CoCr ASTM 75 (39 HRC). However, it is remarks that the depth of LRM layer in each LRM specimens were different as reported in Fig.20. Then, micro-hardness tests were conducted at the center of LRM layers in the cross-sectional area and results are shown in Fig.24. The micro-hardness numbers shows the same trend as micro-hardness numbers where the LRM process resulted in lower hardness value compared to SLM specimens and still higher than casting specimen.

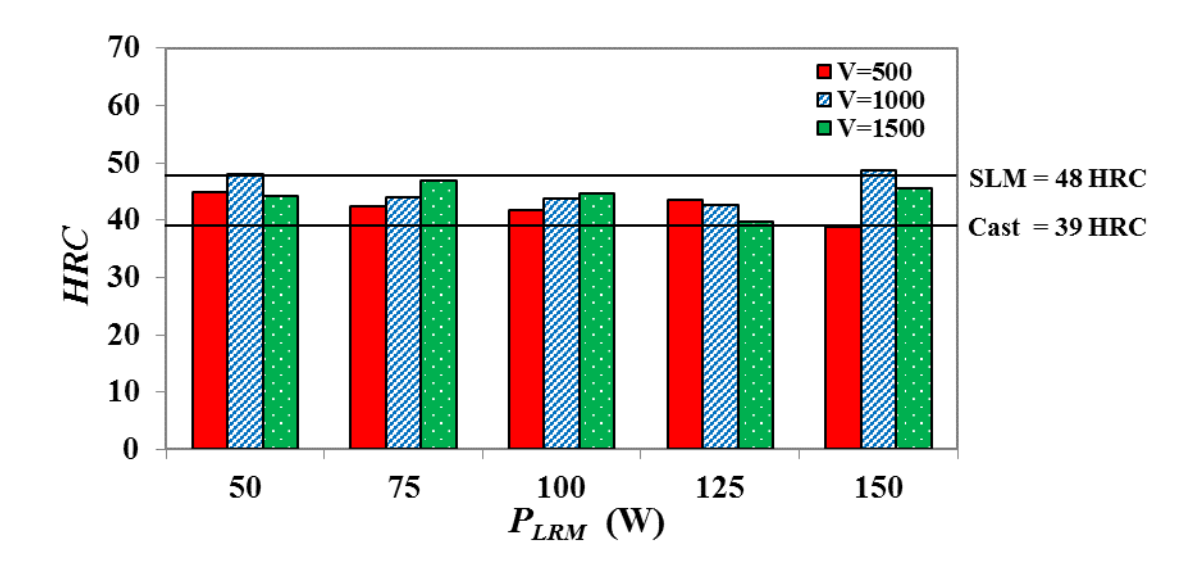


Fig.23 Average macro-hardness (HRC) of SLM and LRM specimens.

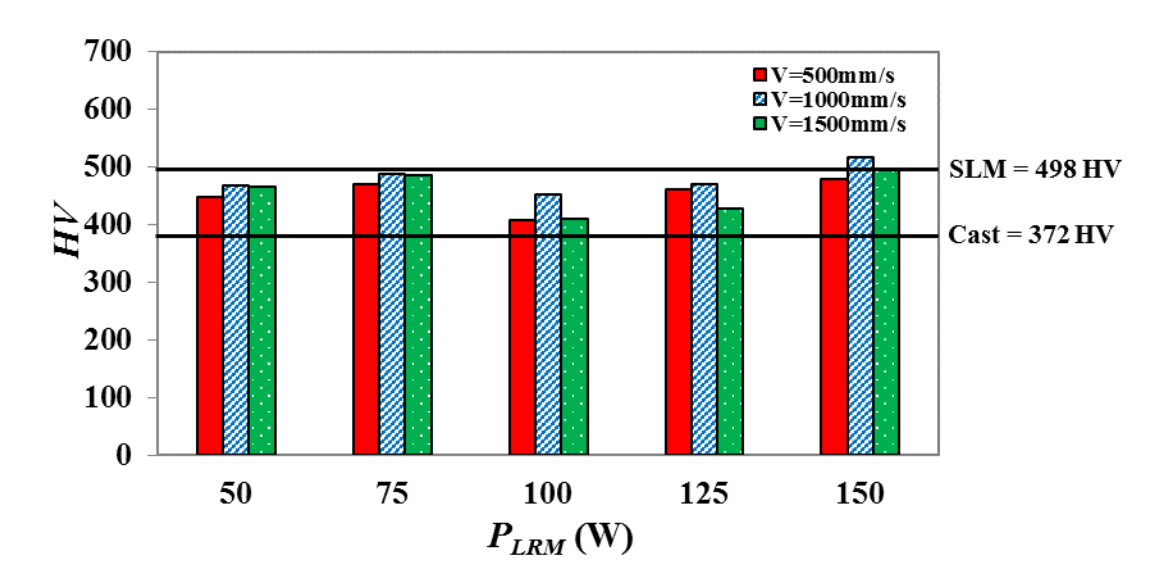


Fig.24 Average micro-hardness (HV) of SLM and LRM specimens.

4.2.3 Dimension

During the LRM process, SLM surface was melted and modified by laser and may lead to the change of dimension. Then, the effect of LRM process on the specimen dimension was investigated using a Coordinate Measuring Machine (CMM). The height of LRM specimen (P_{LRM} =150 W, V_{LRM} =1000 mm/s) was compared with the height of SLM specimen. It was found that the height of LRM specimen reduced by 11.8 μ m. This value agrees with the value measured in cross sectional area as shown in Fig.25 that is about 12 μ m. From this result, we can see that there was a slight decrease in the height of LRM specimen compared to SLM specimen. However, the difference of height depends on the LRM conditions.

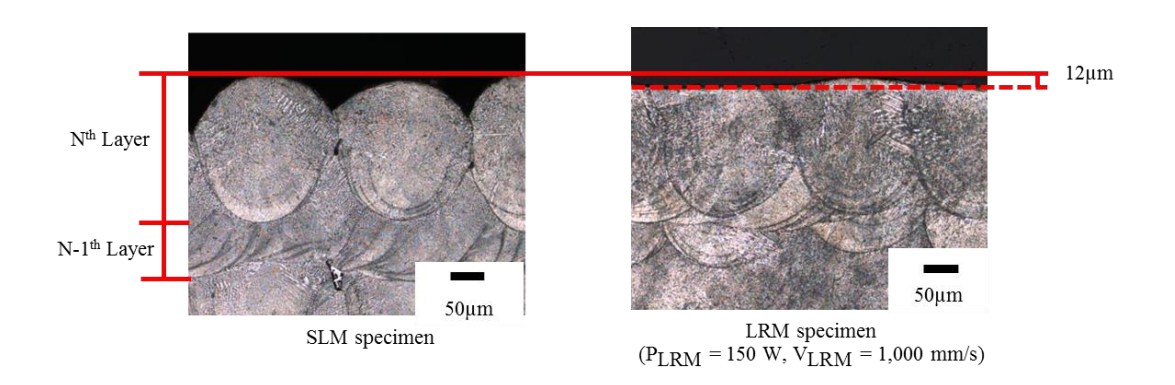


Fig.25 Comparison between the cross-sectional area of SLM and LRM (P_{LRM} =150 W, V_{LRM} =1000 mm/s) specimens.

4.3 The effect of scanning number of LRM process

LRM specimens were fabricated with different repeated numbers of LRM process and results are described as the following discussion.

4.3.1 Surface and cross-sectional area observation

Surface observation of LRM specimens with different repeated numbers of LRM scan were shown in Table 12. According to the results, the surface patterns showed in two patterns. At lower power (P_{LRM} =50W), mesh-liked pattern was

Table 12 The surface observation of LRM specimens in the different scanning number by using scanning electron microscope (SEM).

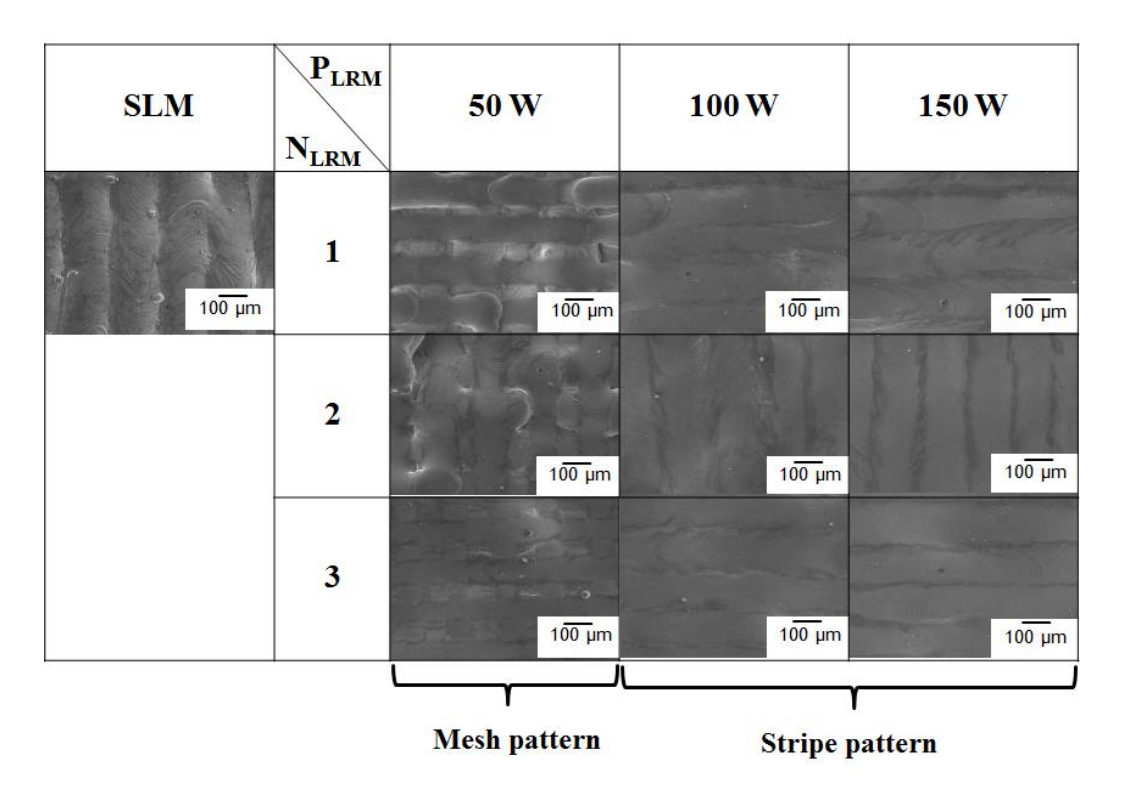
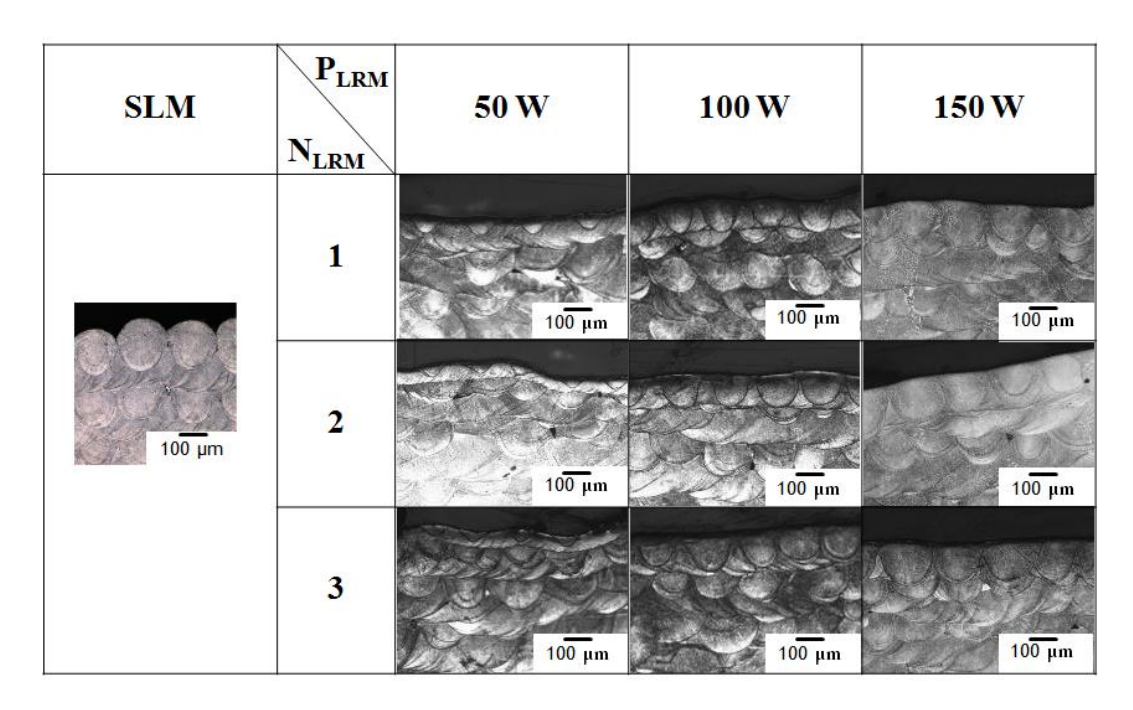


Table 13 The cross-sessional area of LRM specimens in the different scanning number by using scanning electron microscope (SEM).



found at every repeated number of LRM. At $P_{LRM} \ge P_{SLM}$, the LRM surface is strip-liked pattern.

Considering the cross-sectional area in Table 13, the width and the depth of melting pools were measured and shown in Fig.26 and Fig.27, respectively. The melting pools of LRM layer at P_{LRM} =50W were relatively small and the width was less than the hatch spacing value (180 μ m). Each melt pools in this case did not overlap to each other causing mesh-liked pattern in these cases. For stripe-liked pattern, the melting pools overlapped each other as can be seen in the specimen at P_{LRM} >50W. According to the results of depth, it can be recognized that the depth increased with increasing in the scanning number. This may be due to higher accumulated heat induced larger depth when increasing scanning numbers of LRM.

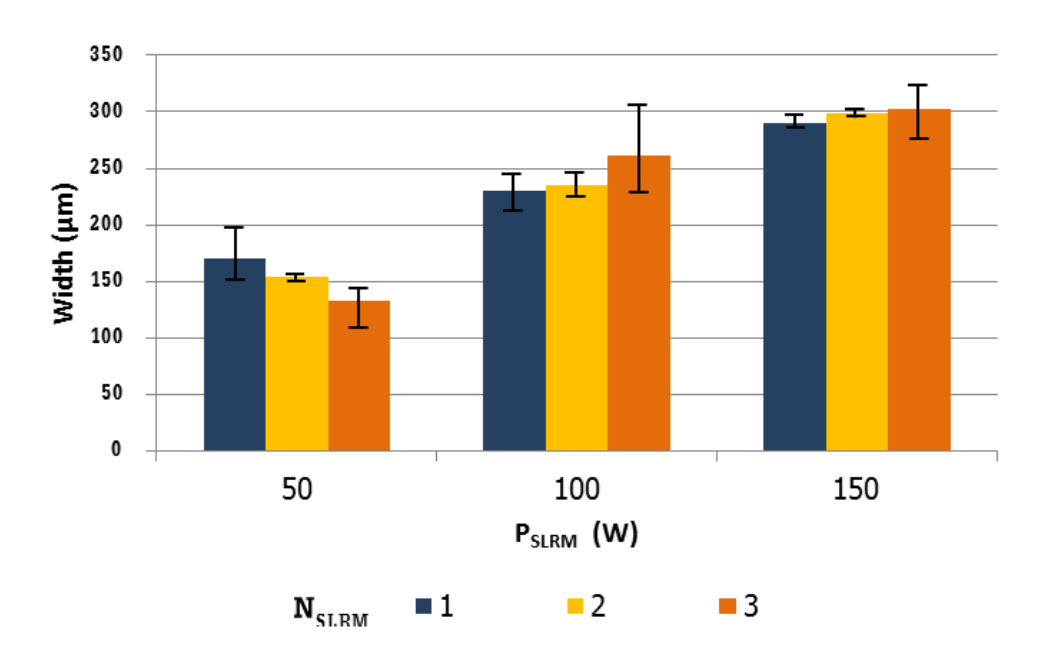


Fig.26 The average width of LRM lines in the cross-sectional area in the different scanning numbers of LRM process.

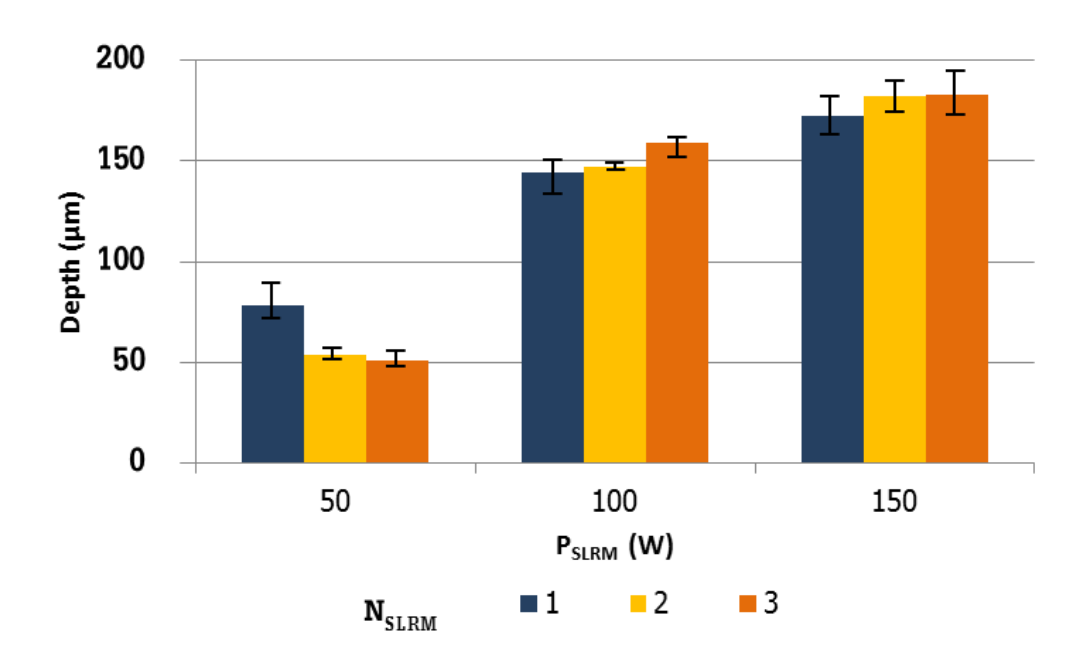


Fig.27 The average depth of LRM lines in the cross-sectional area in the different scanning numbers of LRM process.

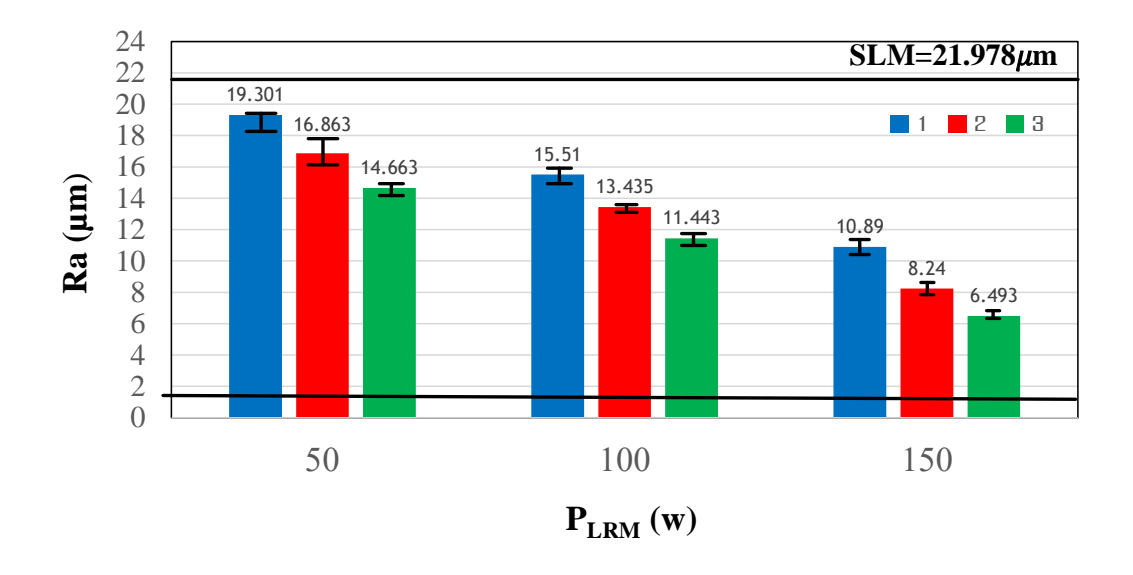


Fig.28 The average surface roughness of LRM specimens at the different scanning numbers of LRM process.

4.3.2 Surface roughness

Surface roughness was measured and presented in Fig. 28. It is obvious that the increase of scanning number caused lower in roughness. The percentage of roughness reduction was calculated and plotted in Fig.29. The reduction rate is high when LRM was applied for first time. Later, the roughness reduced by about 10% at each repeated scanning of LRM process. From this experiments, it can be seen that if we re-melt SLM specimen at P_{LRM} =150W and V_{LRM} =1000 mm/s for 3 times, the roughness can be reduced by 70% to about 6.493 μ m.

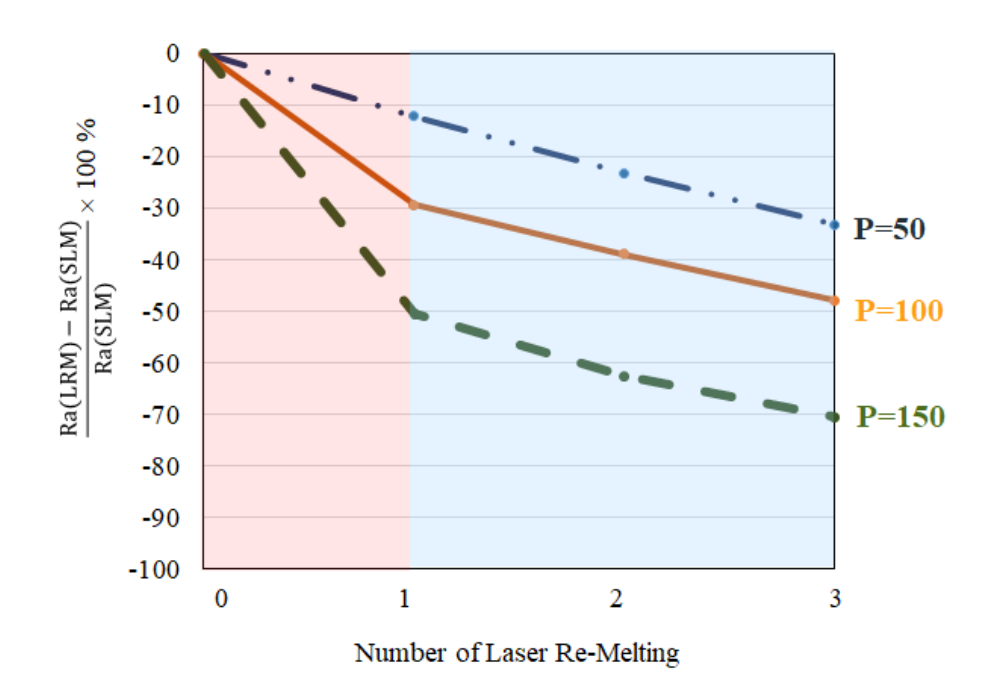


Fig.29 The percentage of roughness reduction compared with SLM specimen.

4.4 Wear behavior

Figure 30 shows the appearance of wear disks after wear test. There are wear debris generated near wear track. According to Table 6, Wear area of casted disk can be easily seen compared to wear area of SLM disk. Moreover, there are amount of debris embedded on the alumina ball where there are no evidence that

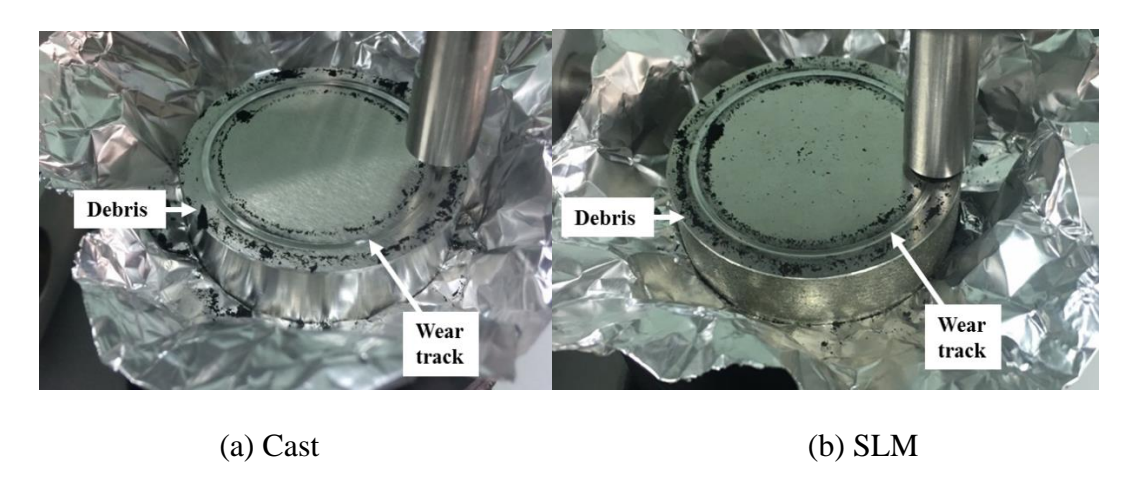


Fig.30 Appearance of (a) casted and (b) SLM disk after wear test.

alumina balls were worn during the test. For these reason, the wear disks and balls were measured the change of eight before and after test, then the mass loss can be plot in the Fig. 31. This can be the evidence that wear occurred mostly on disk side and there is almost no wear occurred on alumina ball side. Moreover, wear rate (W) can be calculated using the following equation;

$$W\left(mm^3/m\right) = \frac{V\left(mm^3\right)}{d\left(m\right)} = \frac{\Delta m\left(g\right)}{\rho\left(\frac{g}{mm^3}\right) \times d(m)}$$
 (Eq.1)

where the density (ρ) of casted CoCr, SLM CoCr and alumina are 0.00841, 0.0083 and 0.0034 g/mm³ respectively. Wear rate are calculated and shown in

Fig.32. Wear rate of SLM is about 2.04 mm³/m which is relatively lower than that of casted specimen. In addition, hardness tests were conducted at testing disk as shown in Fig.33. This reveals that hardness of SLM is slightly greater than casting which may affect to the difference of wear resistance.

Table 14 SEM image of surface appearance after wear test.

Specimens			
	Disk	Ball	Debris
Casting	Wear direction Wear track Base material MTEC3490 20 0ky 10 2mm x80 SE 100 µm	Wear direction Debris embedded on contact area Base material Al ₂ O ₃ 100 µm	1 μm
SLM	Wear direction Wear track Base material MTECM400 20 DAV 10 4mm x50 SE	Wear direction Debris embedded on contact area Base material Al ₂ O ₃ 100 µm	1 μπ

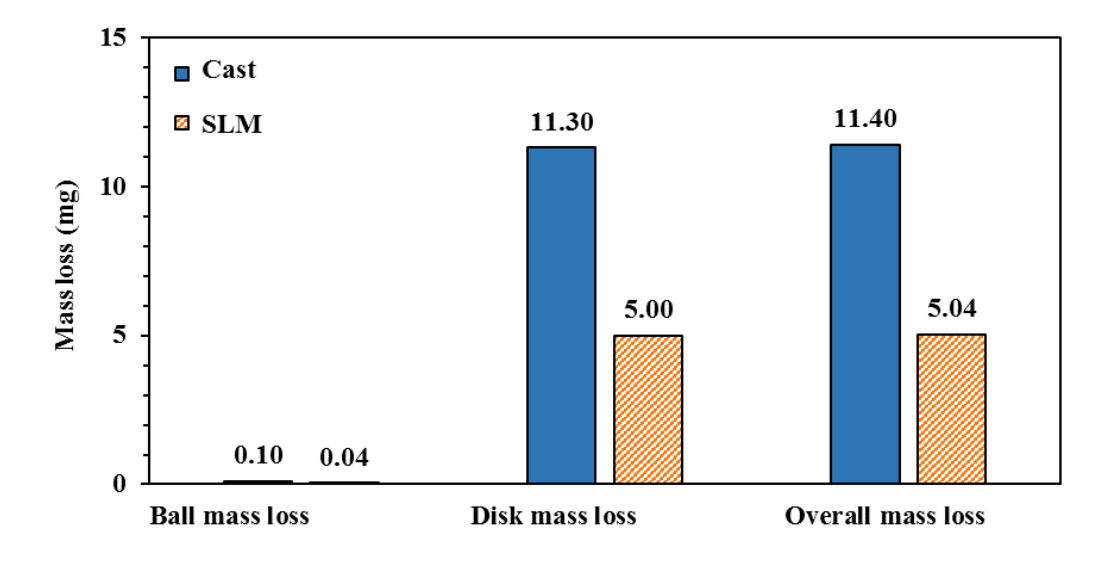


Fig.31 Mass loss due to wear test.

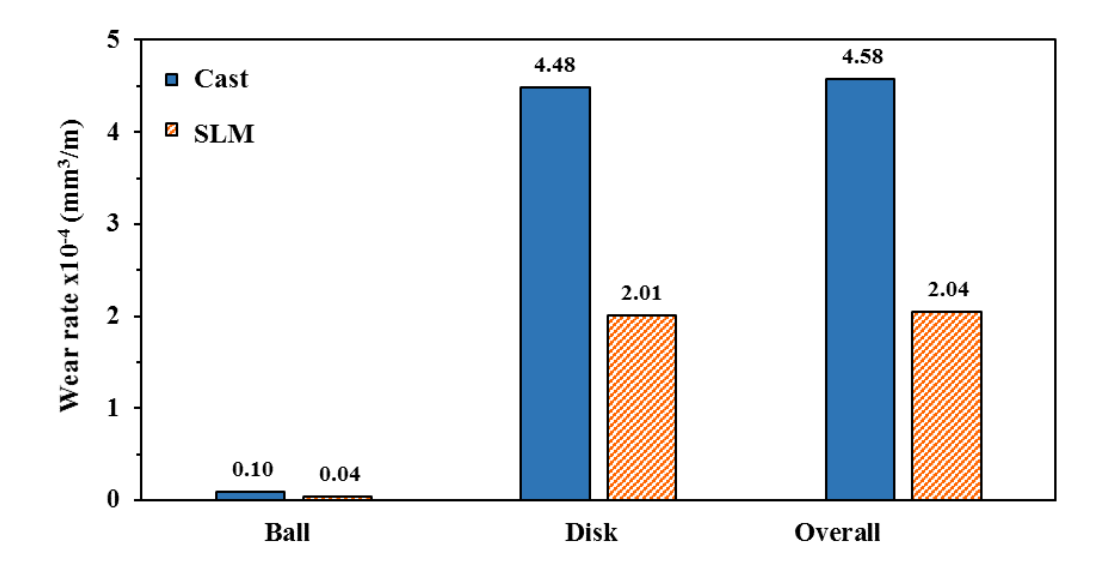


Fig.32 Wear rate

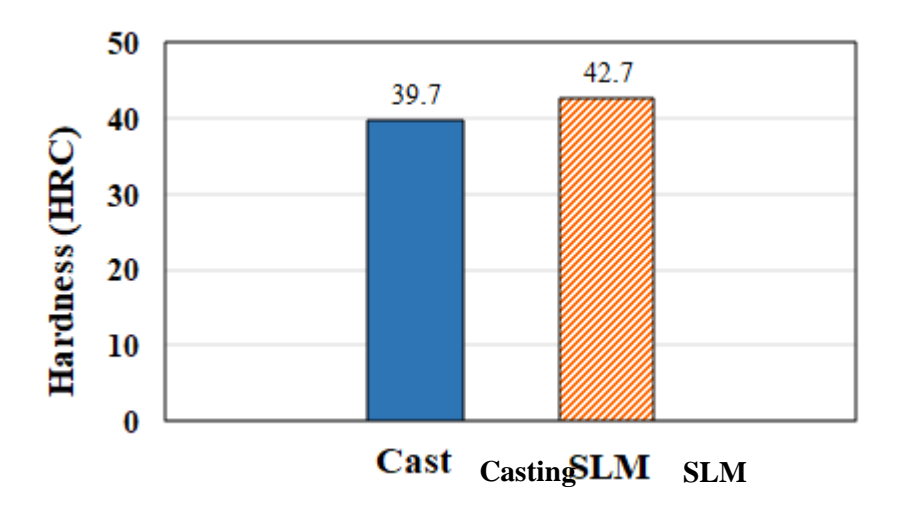


Fig.33 Hardness of casted and SLM disk.

During wear tests, the profile of the friction coefficient (μ) between Alumina ball and casted disk were measured as shown in Fig.34 and the average friction coefficient was about 0.432 which is higher than that of SLM. The average friction coefficient between alumina ball and SLM disk was 0.405. Higher friction coefficient results in higher wear rate in casting specimen. In addition, the penetration depth was measured where the zero setting point is at the

contact point between ball and disk. We can see that the penetration depth along wear tests were different between SLM and cast conditions as shown in Fig.35.

Total penetration depth for casted disk reached to $5.434~\mu m$ while it was only 3.413 for SLM disk. After experiment, disks were well cleaned and measure the depth at wear track using a confocal microscope. It is obvious that the depth of

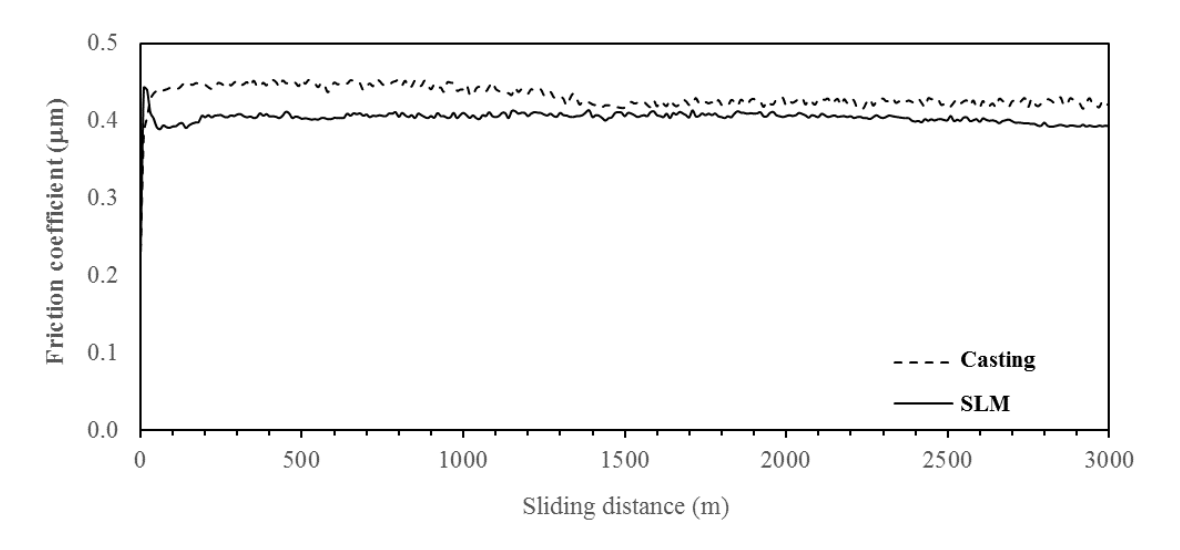


Fig.34 Friction coefficient between alumina ball and tested disks.

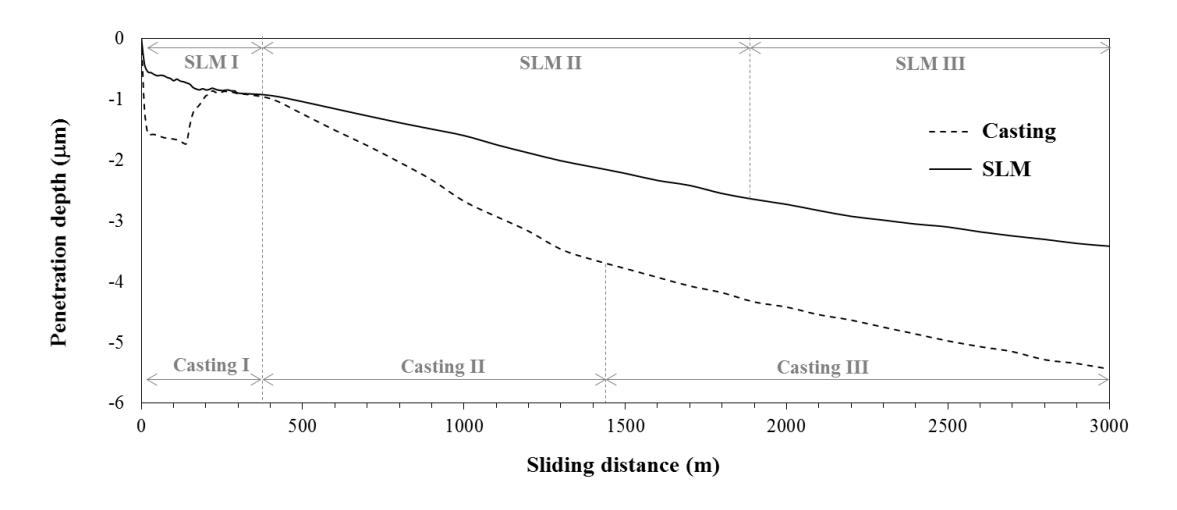


Fig.35 Penetration depth during wear test.

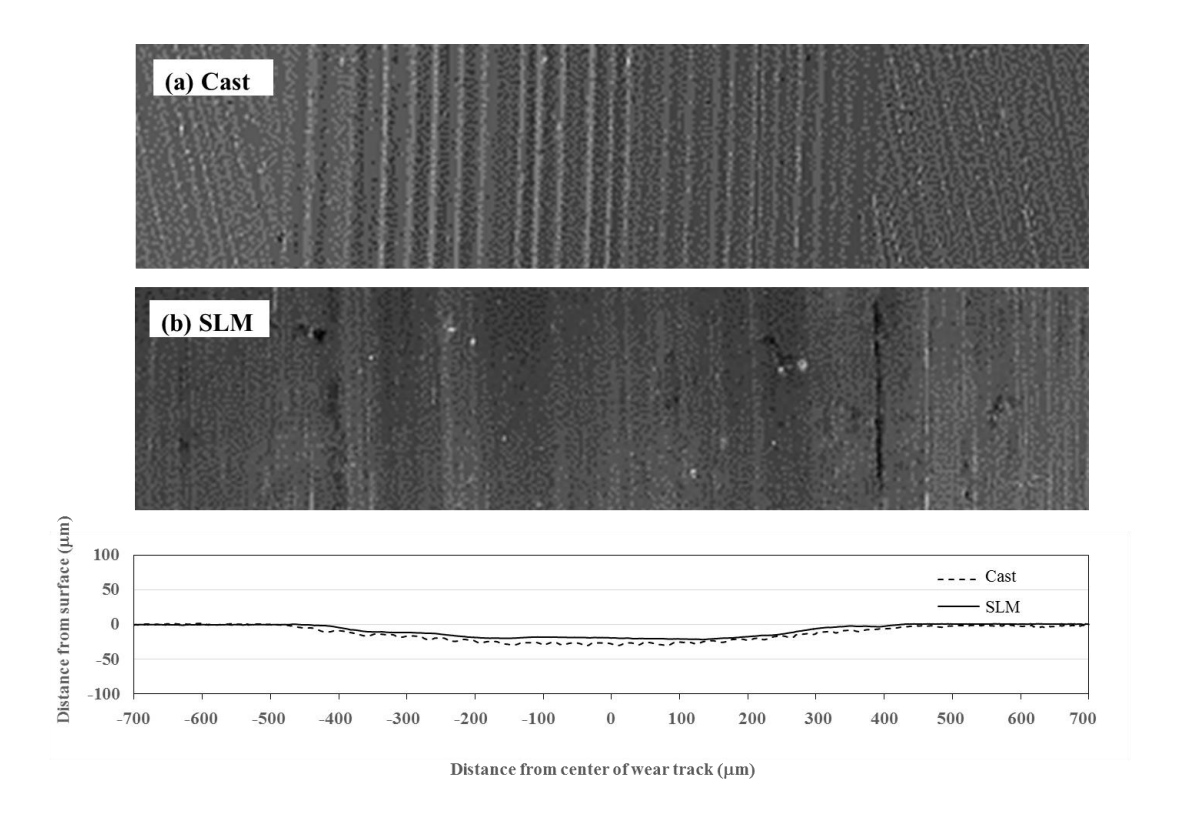


Fig.36 Surface condition and profile across wear track.

wear tracks reached to almost 20 and 30 for SLM and casting, respectively, as shown in Fig.36. The depth of wear track during the test are less than direct measurement due to the debris accumulated between ball and disk. However, we can discuss the wear behavior from the difference in the change of penetration depth in Fig.35.

According to penetration depth, we can recognize that wear behavior can be divided into three stages for both Cast and SLM condition. At first stage, penetration depth suddenly dropped due to the sliding friction between disk and ball as shown in Fig.37. Wear mechanism is two-body abrasive at this stage. Later, wear debris were generated and accumulated between the contact area between disk and ball as shown in Fig.38, consequently the penetration depth

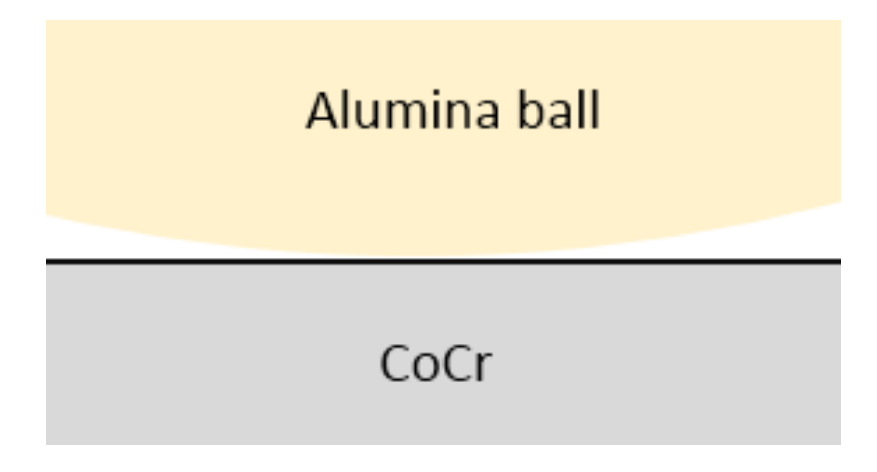


Fig.37 Two-body abrasive wear between alumina ball and CoCr disk.

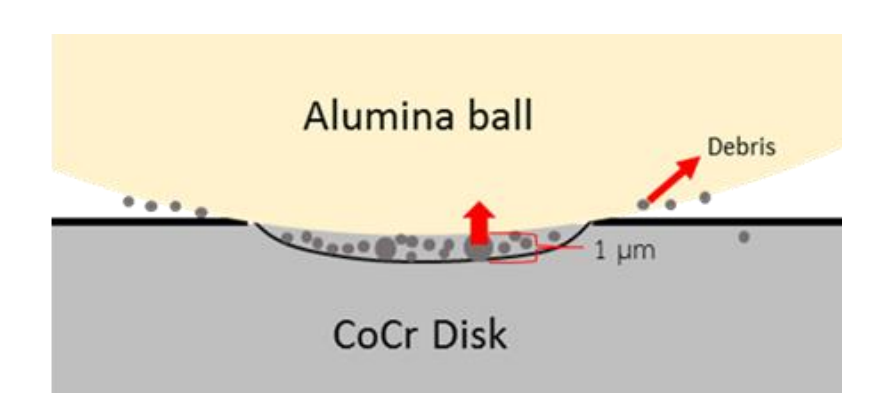


Fig.38 Wear debris generated on the surface of alumina ball and CoCr disk.

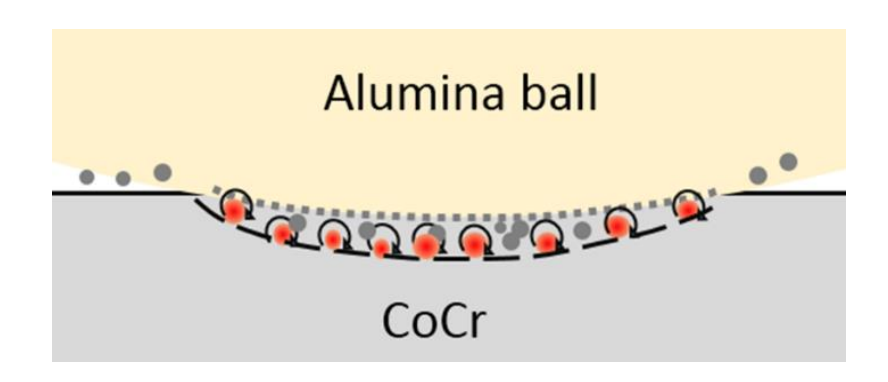


Fig.39 Three-body abrasive wear between alumina ball-CoCr disk-wear debris.

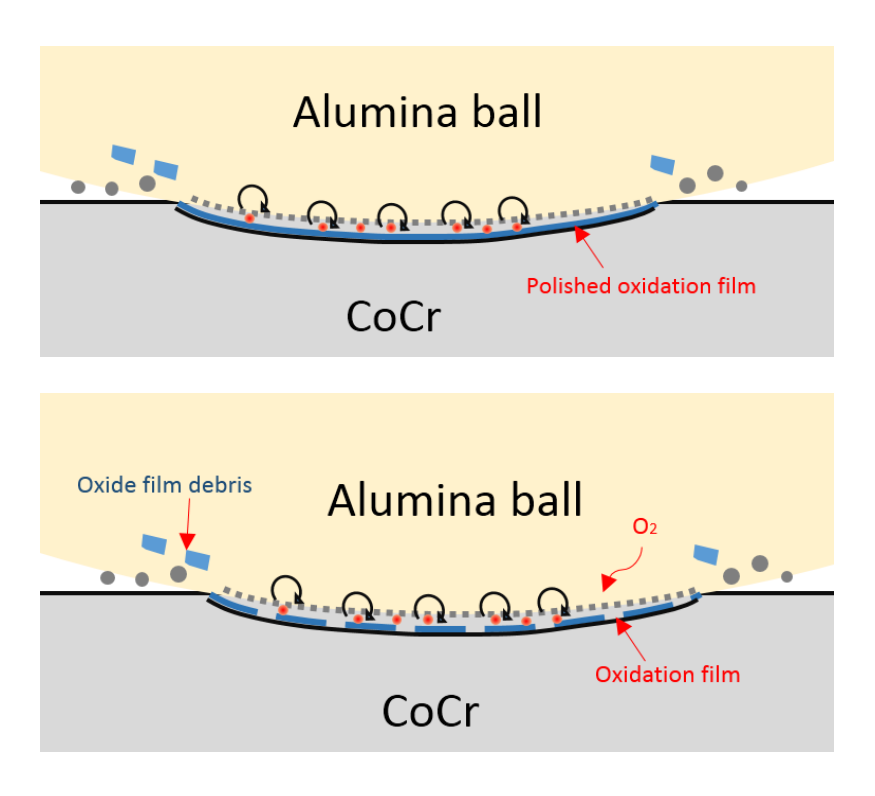


Fig.40 Fretting wear

reveals different wear rate. Wear rate becomes higher at the second stage. At this stage, wear debris might rolled between the contact surface and this may lead to the acceleration of wear rate (Fig.39). Therefore, the causes of wear came from sliding friction due to the contact of ball and disk and rolling friction of wear debris between the surface of ball and disk. During wear test, the heat accumulated on the wear track surface and lead to oxidation at this stage. Thin metal oxide (M_xO_y) layer was formed on the wear track caused the reduction of wear rate as shown in Fig.40. As the disk was subjected to wear load, thin oxide layer broke and release as debris then the new layers were formed again. The evidence of oxygen on wear track were shown in Table 15 and Table 16. The wear mechanism of this stage is fretting wear.

Table 15 Material analysis of casted CoCr disk and wear debris.

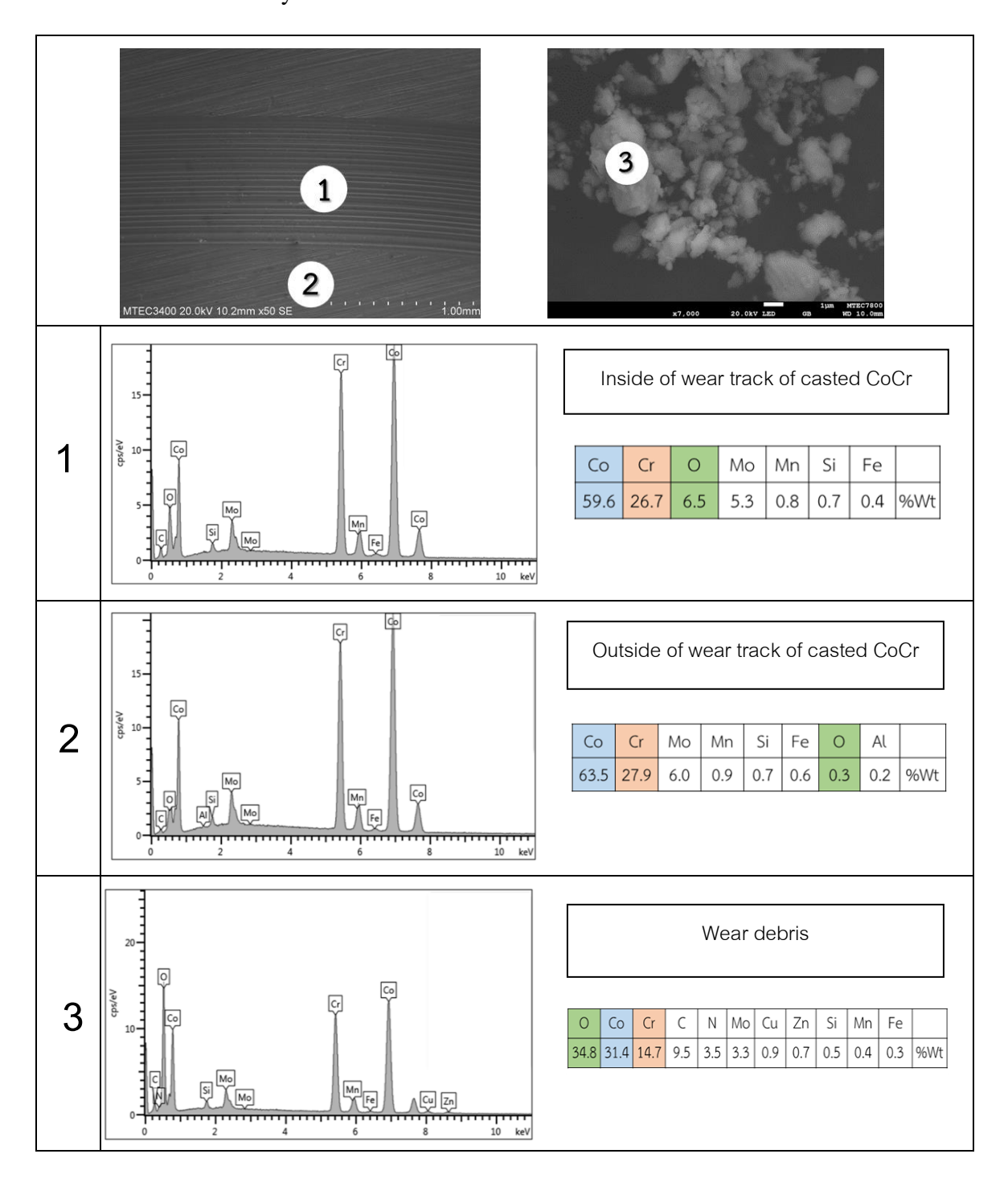
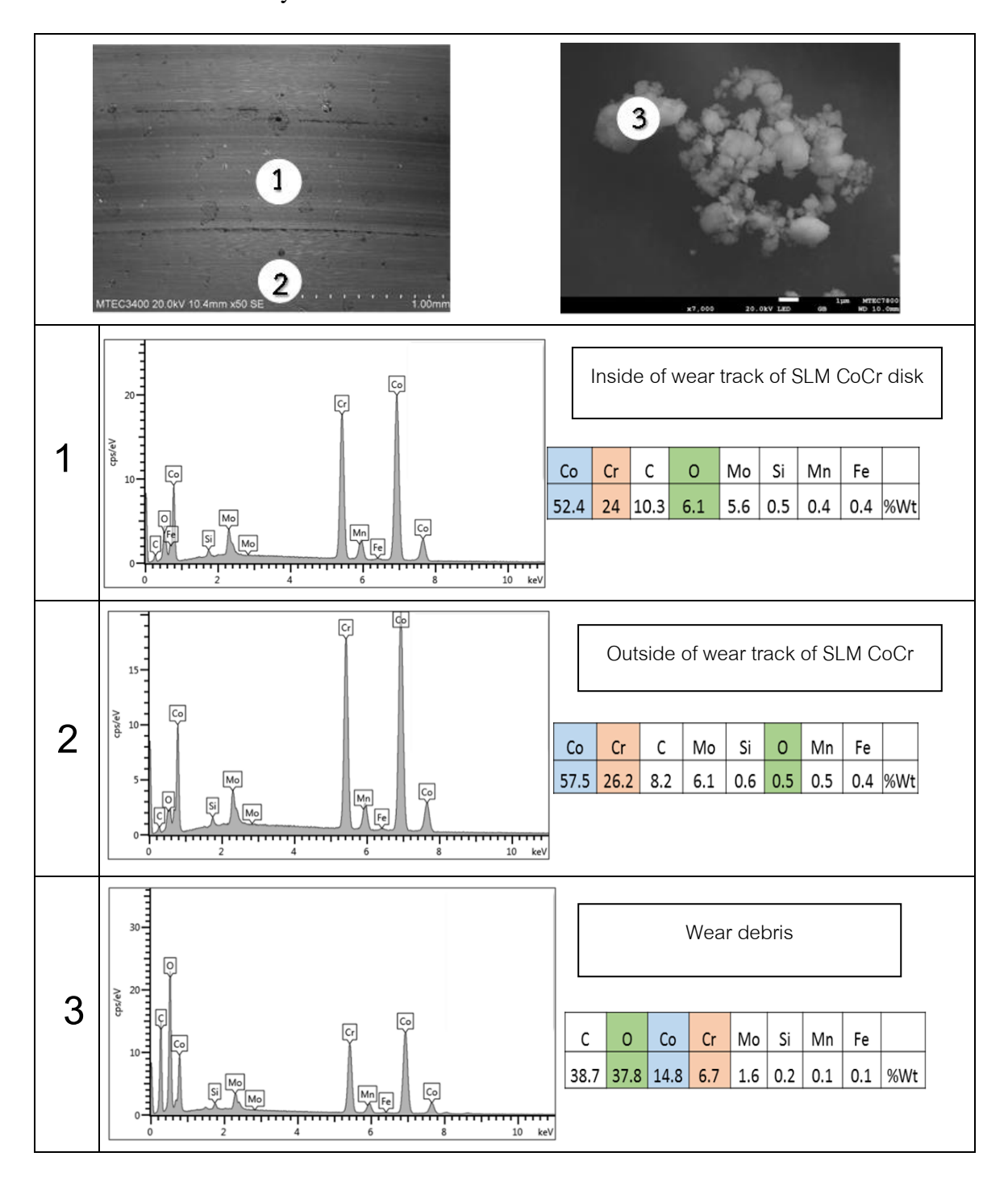


Table 16 Material analysis of SLM CoCr disk and wear debris.



5. Conclusion

This research aims to apply a laser re-melting (LRM) technique to improve surface conditions of Cobalt Chromium (CoCr) alloy after the selective laser melting (SLM) process. The effect of scanning direction, laser processing parameters and scanning number of LRM process on the surface quality of SLM specimens were examined in this study. Moreover, surface roughness, mechanical properties and wear resistance of LRM specimens were also investigated to understand the behavior of CoCr alloy after LRM process. CoCr alloy used in this study is CoCr ASTM F75 powders sized from 20 to 45 µm with the average particle size of 36 µm. Selective Laser Melting (SLM) machine is the National Metal and Materials Technology Center (MTEC)'s self-developed SLM apparatus with a fiber laser. In order to understand the effect of LRM process, LRM process was applied on the top surface SLM specimens in the N₂ environment. SLM specimens were built into the dimension of 10×10×5 mm³ in the conditions of a laser power (P_{SLM}) of 100 W, scanning speed (V_{SLM}) of 1000 mm/s, hatch spacing (H) of 180 µm and the layer thickness (t) of 100 µm. The laser re-melting process were applied on the top surface of SLM specimen in the laser re-melting power (P_{LRM}) from 50-150W and the laser re-melting scanning speed (V_{LRM}) from 500-1500W, while the hatch spacing was fixed at 180 µm. The scanning direction of LRM process was varied at 0°, 45° and 90° to the top layer's fabrication direction (Nth layer direction) of SLM specimen. It was found that LRM in 90° to Nth layer direction performed the best conditions to reduce the surface roughness of SLM among three conditions.

In the next step, the effect of laser power and scanning speed of LRM process were investigated when applied LRM in the cross direction (90°) to Nth layer direction of SLM specimens. It is clear that LRM process enhanced the surface quality by reducing the surface roughness number. Laser re-melting power (P_{LRM}) is recommended to be equal or more than the laser power used for SLM (P_{SLM}). When P_{LRM} is equal or more than P_{SLM}, it could induce sufficient heat to melt all the surface of SLM specimen. Lower P_{LRM} caused discontinuous LRM area resulting in the mesh-liked surface texture and poor roughness. For laser remelting scanning speed (V_{LRM}), it was found that V_{LRM} should be set to be equal to V_{SLM} to give the lowest in the surface roughness. According to the results, the LRM condition at P_{LRM}=150W and V_{LRM}=1000 mm/s could reduce the surface roughness of SLM specimen by 45% from about 21.99 to 11.98 µm. The reduction of roughness leads to the question of the specimen dimension error due to LRM process. For this reason, the height between SLM and LRM (P_{LRM}=50W and V_{LRM}=1000 mm/s) specimens were compared using a coordinate measuring machine (CMM). From the results, we can see that there was a slight decrease in the height of LRM specimen compared to SLM specimen by about 11.8 µm. This error value agrees with the reduction of surface roughness value. However, the dimension of printed part can be later compensated by adding this error value into the design of part before printing by SLM process. In addition, repeating LRM process for several times proved to reduce the surface roughness. In the case of LRM process at P_{LRM}=150W and V_{LRM}=1000 mm/s, the surface roughness reduced by 10% every time increasing scanning number from 1 to 3 times. When LRM process was repeated on SLM specimen for 3 times, the roughness reduced by 70% from 21.99 to 6.49 µm. Moreover, the LRM layer was observed in the cross-sectional area and was found to be very thin layer with the thickness less than 200 µm. However, there was a drop in the hardness value in LRM region compared with a core material of SLM specimen but it was still higher than that of a commercial casted CoCr alloy. Therefore, the change of hardness may affect to the wear behavior of LRM CoCr alloy. Then, the ball-on-disk wear tests were conducted to compare wear resistance between a commercial casted CoCr alloy, SLM CoCr alloy and LRM CoCr alloy. With technical problem, LRM wear specimen was unable to fabricate, therefore the wear tests were conducted only for a commercial cast CoCr alloy and SLM CoCr alloy. Referring to the results, SLM CoCr alloy showed better wear resistance compared with a commercial casted CoCr alloy. This agrees with the result of the hardness value which SLM CoCr alloy show higher in hardness compared with casted CoCr alloy. Since the hardness value of LRM specimen was less than SLM specimen but still higher than casted specimen, therefore there is a possibility that the wear resistance of LRM CoCr alloy might be less than SLM CoCr alloy and higher than casted CoCr alloy. This issue needs to be clarified in the further study.

6. Acknowledge

The author gratefully acknowledge the financial support provided by the Thailand Research Fund. This work would not have been possible without all support from the Medical Device Laboratory, the National Metal and Materials Technology Center (MTEC). Special thanks to Dr. Kriskrai Sitthiseripratip, Dr.

Passakorn Tesavibul, Dr. Prasert Chalermkarnnon and Mr. Pongnarin Jiamwatthanachai who provided expertise that greatly assisted this research work. The author would especially like to thank Professor Dr. Chaosuan Kanchanomai and Associate Professor Dr. Yukio Miyashita, the mentor of this project for their thoughtful comments and efforts towards improving this research. Finally, the author would like to thank you all support from all students in the Metallurgical and Material Engineering Laboratory, Department of Industrial Engineering, the Faculty of Engineering, Thammasat University.

7. References

- [1] Eleftherios Louvis, Per Fox and Christopher J. Sutcliffe, Selective Laser Melting of aluminium components, *Materials Processing Technology*, 211, 2011, pp.275-284.
- [2] K. Kempen, L. Thijs, J.Van Humbeeck and J.-P. Kruth, Mechanical Properties of AlSi10Mg Produced by Selective Laser Melting, *Physics Procedia*, 39, 2012, pp.439-446.
- [3] Jared R. H. Foran, MD, Total Hip Replacement, *Ortho Info Website* (http://orthoinfo.aaos.org), August 2015.
- [4] Christian Fabry, Carmen Zietz, Axel Baumann and Rainer Bader, Wear Performance of Sequentially Cross-Linked Polyethylene Inserts against Ion-Treated CoCr, TiNbN-Coated CoCr and Al2O3 Ceramic Femoral Heads for Total Hip Replacement, *Lubricants* 2015, 3, 2015, 14-26;
- [5] I. Yadroitsev and I. Smurov, Surface Morphology in Selective Laser Melting of Metal Powders, Physics Procedia, 12, 2011, pp.264-270.
- [6] A. Temmler, E. Willenborg and K. Wissenbach, Laser Polishing, *Proceedings* of SPIE The International Society for Optical Engineering, 2012.

- [7] E. Yasa, J.-P. Kruth and J.Deckers, Manufacturing by combining Selective Laser Melting and Selective Laser Erosion/Laser Re-Melting, *CIRP Annals-Manufacturing Technology*, 60, 2011, pp.263-266.
- [8] E. Yasa and J.-P,Kruth, Application of Laser Re-melting on Selective Laser Melting Parts, Advances in Production Engineering & Management, 6, 2011, 4, pp.259-270
- [9] Costel-Relu Ciubotariu, Doina Frunzăverde, Gabriela Mărginean, Viorel-Aurel Şerban and Aurel-Valentin Bîrdeanu, Optimization of the laser remelting process for HVOF-sprayed Stellite 6 wear resistant coatings, *Opticals & Laser Technology*, 77, 2106, pp.98-103.
- [10] I. Gotman and E. Y. Gutmanas, Wear-Resistant Ceramic Films and Coatings, Comprehensive Biomaterials; Metallic, Ceramic and Polymeric Biomaterials, Volume 1, Elesevier Science, Amsterdam, The Netherlands, 2011, pp.127-155.
- [10] N. Pagano, V. Angelini, L. Ceschini, and G. Campana, Laser Remelting for Enhancing Tribological Performances of a Ductile Iron, *Procedia CIRP*, 41, 2016, pp.987-991.

8. Output from this research project

- A paper submitted to the international journal is under review.